.

To my farher and mother
who were, are, and ever will be
the source of inspiration
along my ongoing journey of success.

Abstract

The mechanical pulp bleaching process at Irving Paper is mostly manually controlled, which degrades the quality of the produced paper due to the variations in the pulp brightness. The objective of this research was to study the possibility of controlling the pulp bleaching process at Irving Paper mill. This would improve the pulp quality by minimizing the final pulp brightness variability, and achieve some economical benefits by minimizing the consumption of the bleaching chemicals. The bleaching process was thoroughly studied and modelled in this research. A delay time estimator was designed to tackle the problem of the long variable delay time, which is considered the biggest challenge in this process.

The model predictive control (*MPC*) strategy is chosen to control the bleaching process taking into account the constraints, which are imposed by the operating conditions of the process itself. In order for the *MPC* controller to handle such constraints , a state of the art of optimization method, i. e. an interior point method was incorporated in the controller. The designed *MPC* controller formed a basis for an industrial control prototype. The control technology was designed and implemented in the real-world bleaching process at Irving Paper mill, in order to test and demonstrate the performance of the *MPC* controller in real time. This, in turn, demonstrated the closed loop behaviour of the bleaching process itself in real time.

Acknowledgement

I would like to express my profound gratitude and high regards to professor James H. Taylor, my research supervisor, his encouragement, friendship, generosity, and inspiring suggestions during the course of this research have played a vital role.

I also would like to express my sincere appreciation to Irving Paper management represented by Dr. Tony Binitto and Mark Mosher, and to its technical team Zhiqing Li, George Court, and all those who worked behind the scenes. Their great support, impressive cooperation, and invaluable discussions have enhanced this research and have led to its success.

Many thanks go to Dr. Yonhgao Ni in the Pulp and Paper Research Center at UNB, his informative discussions and suggestions are highly appreciated.

Sincere appreciation is extended to the faculty and staff of the Department of Electrical and Computer Engineering at UNB for their patience and continuous encouragement.

I would like to thank my father, mother, and my family for their enormous patience, unlimited support and profound encouragement.

Contents

1 The Technology of Mechanical Pulp Bleaching **1**

1.1 Introduction 2

1.2 General description of peroxide bleaching processes 2

1.3 Factors affecting brightness response in peroxide bleaching 3

1.3.1 Effect of initial brightness of wood and unbleached pulp . . . 3

1.3.2 Effect of the pulping process on initial brightness 4

1.3.3 Effect of metal impurities 5

1.3.3.1 Pretreatment of mechanical pulp with organic chelants 5

1.3.3.2 Stabilization of peroxide bleach liquor with sodium silicate 5

1.4 Process variables 6

1.4.1 Peroxide charge 6

1.4.2 Total alkalinity pH 6

1.4.3 Consistency 7

1.4.4 Time and temperature 9

2 The Identification of Mechanical Pulp Bleaching Dynamics **10**

2.1 Introduction 11

2.2 Mathematical modelling of the bleaching process 11

2.3 System identification of the bleaching process 12

2.4 Practical aspects 13

2.4.1 Delay time estimation 16

2.4.2 Model parameter estimation 17

2.5 The SO_2 effect on the brightness response 22

3 Controller Design **24**

3.1 Model predictive control 25

3.2 Dynamic matrix control 26

3.2.1 Prediction 26

3.2.2 Measurable disturbances 28

3.2.3 Objective function 28

3.2.4 Reference trajectory 29

3.2.5 The unconstrained *DMC* case 30

3.2.6 The constrained *DMC* case 30

3.3 The effect of penalizing the control moves 31

3.4 *DMC* strategy for variable delay-time systems 33

4 Optimization Algorithms For Convex Quadratic Programming **36**

4.1 Introduction 37

4.2 Convex quadratic programming 37

4.3 Active set method for convex QP 39

4.4 Interior point methods 40

4.5 Mehrotra predictor corrector algorithm for convex QP 42

4.6 Hot starting 46

4.7 Interior point methods vs. active set methods 46

5 Simulation and Implementation Results **48**

5.1 The bleaching process controller design issues 49

5.2 Nominal performance 51

5.3 Robust performance 53

5.4 Implementation results 58

5.4.1 *DMC* controller test: objectives and difficulties 58

5.4.2 First test results 59

5.4.3 Discussion and analysis of the first test results 60

6 Thesis Observations **65**

6.1 Summary and conclusions 66

6.2 Future work 68

A Brightness Principles and Measurement **74**

A.1 Meaning and interpretation of brightness 75

A.2 Brightness and chromophore concentration 75

A.3 Brightness standards 76

A.4 Brightness sensors 77

B Test and Implementation Issues **79**

B.1 Test and experiment details 80

B.1.1 The graphic user interface (*GUI*) part 81

B.1.2 The database and run time engine parts 82

List of Figures

1.1 Flowsheet for single-stage peroxide bleach plant [1]. 3
1.2 Effect of pulping processes on initial pulp brightness, Stone GroundWood (SGW), Pressurized GroundWood (PGW), and ThermoMechanical Pulping (TMP) [1]. 4
1.3 Effect of DTPA addition on pulp brightness response [1]. 5
1.4 Impact of sodium silicate addition on brightness gain [1]. 6
1.5 Effect of hydrogen peroxide application on pulp brightness [1]. . . . 7
1.6 Influence of $\frac{TA}{[H_2O_2]}$ ratio on pulp brightness [1]. 8
1.7 Effect of consistency on pulp brightness [1]. 8
1.8 The effect of temperature on the rate of brightness development [1]. 9

2.1 Block diagram of the prediction error method. 13
2.2 Flowsheet of the Bleaching process at Irving Paper [2]. 15
2.3 The estimated delay time, first data set. 18
2.4 The estimated and real pulp brightness, first data set. 19
2.5 The estimated delay time, second data set. 20
2.6 The estimated and real pulp brightness, second data set. 21
2.7 The SO_2 effect on pulp brightness. 23

3.1 Forced and free response. 27
3.2 Reference trajectory. 29
3.3 The effect of structuring the control law for the unconstrained case. 32
3.4 The effect of structuring the control law for the constrained case. . 33
3.5 Comparison between variable and constant delay time DMC controllers. 35

4.1 Illustration of convex quadratic programming. 38

5.1 The nonlinear brightness gain with respect to peroxide dosage. . . . 49
5.2 The bleaching process DMC controller. 50
5.3 System response to stairs signal at different delay times 51
5.4 The effect of disturbance rejection on the system performance . . . 52
5.5 The system response to $\mp$20% gain uncertainty. 54
5.6 The system response to $\mp$20% time-constant uncertainty. 55
5.7 The system response to $\mp$5% delay time uncertainty. 56
5.8 The system response to $\mp$10% delay time uncertainty. 57
5.9 The dosages of secondary bleaching chemicals, first test. 60
5.10 The final pulp brightness to a step change at the reference, first test. 61
5.11 The final pulp brightness responses after removing the bias, first test. 62
5.12 The estimated delay time, first test. 63
5.13 The effect of forward delay time estimation on the brightness response, first test. 64

A.1 Different types of light interactions with paper [3]. 75
A.2 Relationship between brightness and chromophore concentration [3]. 76
A.3 Cormec measurement [4]. 77

B.1 The DMC control technology implementation at Irving Paper mill. 81
B.2 The DMC control technology main window. 82
B.3 The GUI design scheme of the DMC control technology. 84
B.4 The run time engine scheme of the DMC control technology. 85
B.5 The flow chart of the control algorithm in the control technology. . 86

1.1 Unbleached brightness of softwood TMP (table) [1]. 4

Chapter 1

The Technology of Mechanical Pulp Bleaching

1.1 Introduction

Pulp brightness is measured as reflectance in the blue portion of the visible spectrum. Complete reflectance provides a white color. Absorption of any part of the visible spectrum by a material will result in the perception of color by the eye. Pulp brightness is measured against a magnesium oxide (MgO) standard on a scale of 0-100, which defines the *ISO* standard. Bleached kraft for example has brightness values ranging from $86 - 94$ *%ISO*, unbleached kraft (brown paper bags) has a brightness of $20 - 30$ *%ISO*, and newsprint is around 55 *%ISO*. Pulp darkness is due to lignin and lignin degradation products, and the specific compounds which cause light absorption (and therefore a colored pulp) are termed chromophores.

There are two basic methods for improving brightness. One can retain the lignin and remove only the chromophores. This is termed pulp brightening. This is not a permanent brightness improvement, as UV light and oxygen will create more chromophores and cause yellowing (reversion). Classical bleaching processes are essentially a delignification reaction in which lignin is removed from the pulp. This results in a permanent brightness improvement. Bleaching is typically done in several stages. Bleaching chemically reduces the concentration of light absorbing constituents so that paper reflects more light. Improved reflectance is both the purpose of the bleaching process and the means of monitoring its progress.

Lignin is generally singled out as the constituent having the greatest direct influence on the colour of wood. The objective in the bleaching of mechanical pulps is to selectively remove the colour-contributing groups while simultaneously preserving a high pulp yield. This involves mainly the use of bleaching agents such as hydrogen peroxide and the sodium hydrosulfite. Hydrogen peroxide is the most widely used oxidative bleaching agent in mechanical pulp bleaching, particularly where high brightness is desired.

1.2 General description of peroxide bleaching processes

The bleaching of mechanical pulp with hydrogen peroxide is usually carried out by pretreating the pulp with pentasodium diethylenetriaminepentaacetic *DTPA* solution (an alkaline solution) to remove transitional metal ions in pulp, then the pulp is mixed with an alkaline peroxide bleaching solution (bleach liquor). The

mixture of pulp and liquor is then held in a bleaching tower for several hours at temperatures that range from 140° to 180°F. After exiting the tower, the pulp pH is lowered to prevent alkaline reversion and decompose the residual peroxide. Then the pulp is sent to the paper machine or to dryers when produced as a market pulp [1]. The typical peroxide bleach plant is the single-stage medium-consistency bleach plant as shown in figure 1.1.

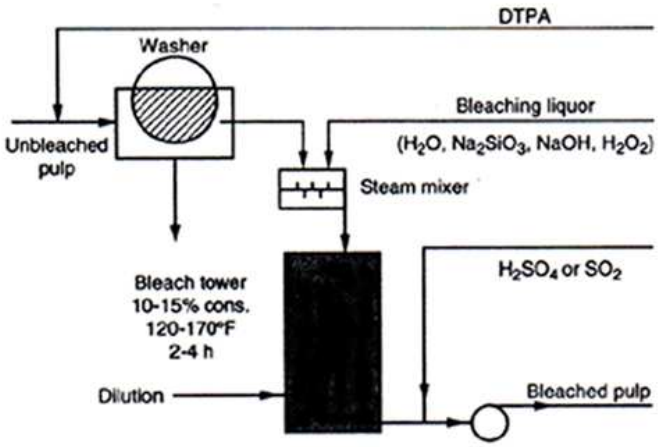

Figure 1.1: Flowsheet for single-stage peroxide bleach plant [1].

1.3 Factors affecting brightness response in peroxide bleaching

The raw material in mechanical pulping is wood. At present mechanical pulps are made from a large variety of both soft woods and hard woods, all of which have different responses in peroxide bleaching. Several factors have a significant impact on the bleachability of the pulp, and in turn determine the desired target brightness of the pulp.

1.3.1 Effect of initial brightness of wood and unbleached pulp

The initial brightness and potential brightness response of any pulp is highly dependent on the wood species from which it is made. The wide range of brightness values found after thermomechanical pulping (TMP) of a variety of softwoods is shown by the data in figure 1.1. Generally a higher initial brightness implies a higher bleached brightness when equivalent amounts of bleaching chemical are applied.

Wood Species	Unbleached *TMP* Brightness, *%ISO*
Black spruce	59.4
Jack pine	59.5
Eastern larsh	41.6
Balsam fir	54.5
Lodgepole pine	56.7
Eastern hemlock	45.2
White pine	57.3
Red pine	61.1

Table 1.1: Unbleached brightness of softwood TMP [1].

1.3.2 Effect of the pulping process on initial brightness

Mechanical pulping refers to a wide variety of processes, but the major mechanical pulping processes employ grinders and refiners to separate the wood fibres. Ground wood pulping processes employ pulp stones at atmospheric temperatures and pressures whereas the refiner pulping typically consists of two or more disc refining stages. Thermomechnical pulping differs from refiner mechanical pulping in that the chips are preheated to a temperature of $120°– 133°C.$, and refined under pressure in the primary refiner. In general, the higher the temperature of the pulping process the lower the relative bleachability of the mechanical pulps made from the same wood species, as shown in figure 1.2.

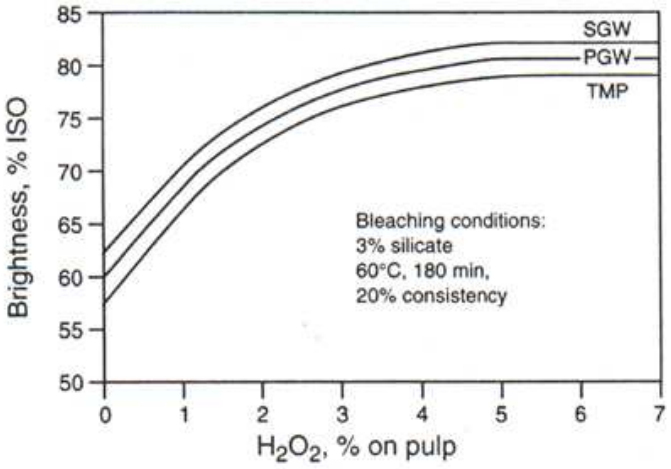

Figure 1.2: Effect of pulping processes on initial pulp brightness, Stone GroundWood (SGW), Pressurized GroundWood (PGW), and ThermoMechanical Pulping (TMP) [1].

1.3.3 Effect of metal impurities

Metals, particularly transition metals, act as catalytic decomposition agents when in contact with hydrogen peroxide. The most common metals routinely encountered in the peroxide bleaching of mechanical pulps are manganese, iron, copper, and nickel. Of these, the most active decomposition element is manganese. The first step in successful hydrogen peroxide bleaching is to minimize the occurrence of catalytic decomposition. Two approaches are used to achieve this goal [1]:

1.3.3.1 Pretreatment of mechanical pulp with organic chelants

The purpose of pretreating mechanical pulps is to complex and wash out most of the transition metals present in the pulp before applying the bleach liquor. The pre-treatment is usually carried out at a pH of $4.0 - 6.0$, using an organic chelant which forms an organo-metallic complex with the free metal. Then the pulp is thickened to medium consistency where the chelated metals are washed from the pulp. The bleach response curve in figure 1.3 shows the effect of adding a common chelant agent, namely $DTPA$, to the pulp.

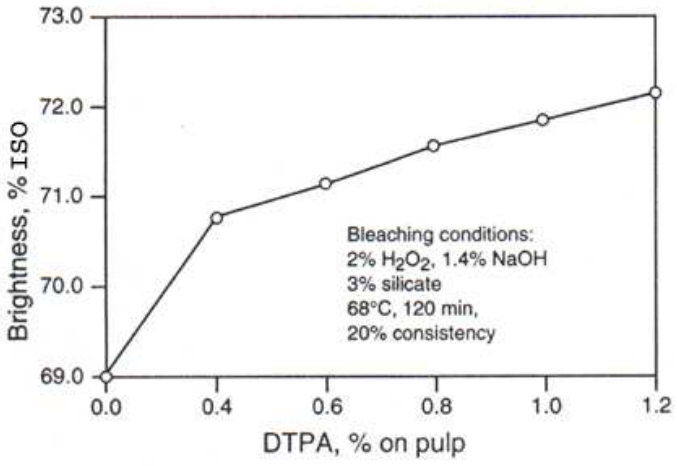

Figure 1.3: Effect of DTPA addition on pulp brightness response [1].

1.3.3.2 Stabilization of peroxide bleach liquor with sodium silicate

Sodium silicate is a cost-effective stabilizer for alkaline peroxide bleaching and produces two strong benefits. It significantly reduces peroxide decomposition oc-

curring during bleaching, and it improves the internal stability of the bleach liquor solution itself. The addition of silicate to the bleach liquor leads to a higher brightness for the same peroxide application as shown in figure 1.4.

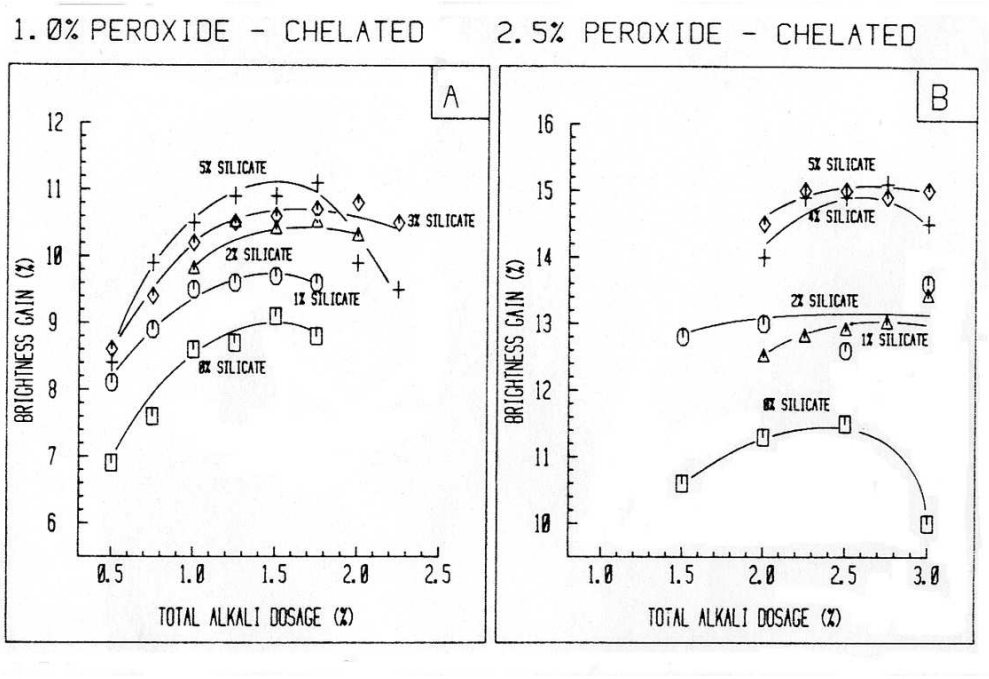

Figure 1.4: Impact of sodium silicate addition on brightness gain [1].

1.4 Process variables

1.4.1 Peroxide charge

Brightness response in the peroxide bleaching of mechanical is directly related to peroxide application. Increased peroxide dosage leads to increased brightness as shown in figure 1.5. However, for a given set of bleaching conditions and furnish, there is a threshold beyond which increased peroxide dosage has a minimal effect on brightness.

1.4.2 Total alkalinity *pH*

The most important relationship for the proper control of alkaline peroxide mechanical pulp bleaching is that between peroxide and alkalinity. If the alkali charge is too low, inefficient bleaching is likely to result; too high an alkali charge may lead to pulp darkening or yellowing.

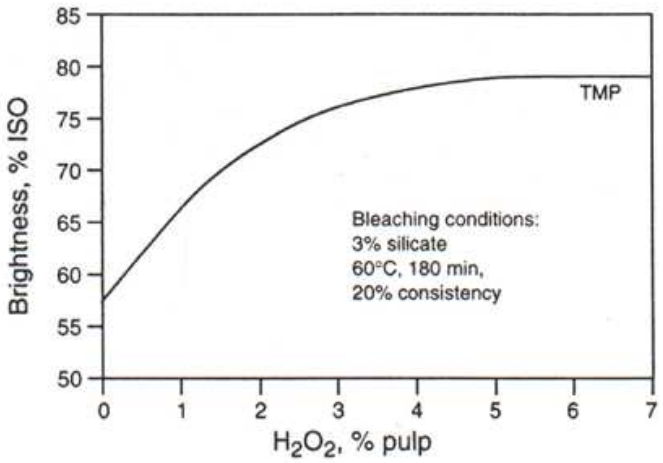

Figure 1.5: Effect of hydrogen peroxide application on pulp brightness [1].

In a peroxide bleaching system, the initial pH of the pulp slurry determines the nature of the bleaching chemical reaction. If the initial pH is too high, the rate of peroxide decomposition may exceed the rate of the bleaching reaction, thereby reducing the brightness response. If the initial pH is too low, the lower perhydroxyl anion concentration impedes the brightness development.

Total alkalinity is the sum of all sources of alkali in the bleach liquor, mainly sodium hydroxide and sodium silicate. The total alkali application can be expressed by:

$$\%Total\ alkali = \%NaOH + 0.115 \times \%Na_2SIO_3 \tag{1.1}$$

A useful way of expressing the relationship between peroxide and total alkalinity (TA) is the $\frac{TA}{[H_2O_2]}$ ratio. The optimum $\frac{TA}{[H_2O_2]}$ ratio decreases as the hydrogen peroxide dosage increases, as shown in figure 1.6. This is partially explained by the alkali demand from the wood acids present in the pulp. Because the alkali demand is constant, it is more significant at low peroxide applications than at high peroxide applications.

1.4.3 Consistency

Pulp consistency is defined as the ratio of the mass of fibrous material in a slurry to the total mass of the wet slurry on a bonedry basis. The consistency of pulp slurries is important to the papermaker since its control directly affects the uniformity of the paper produced [5]. Hydrogen peroxide bleaching can be carried out over a wide

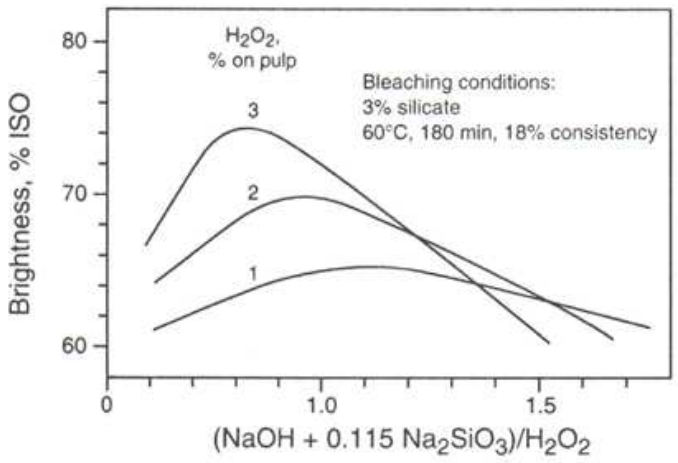

Figure 1.6: Influence of $\frac{TA}{[H_2O_2]}$ ratio on pulp brightness [1].

consistency range, from as low as 4% to as high as 35%. Figure 1.7 illustrates the effect of consistency on bleaching response. It is clear that at low consistency, not only does the pulp require more peroxide to achieve the same brightness, but there is a definite ceiling for the brightness response which can not be exceeded by further peroxide addition. The slope of the response curves for the higher consistency pulps indicates that further brightness gains can be achieved. A continuous increase in bleaching response occurs as consistency is increased up to 40% level.

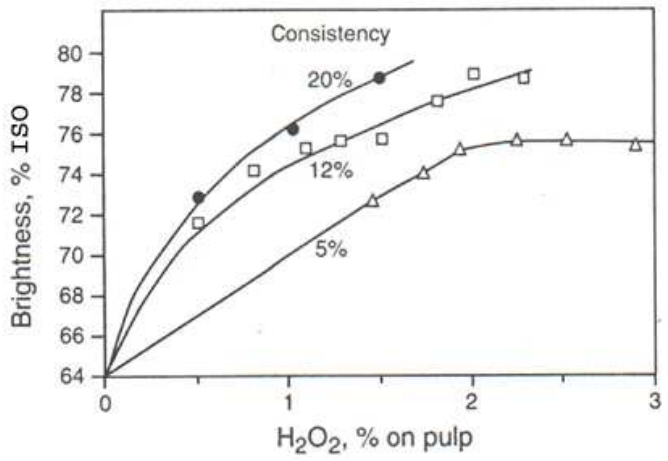

Figure 1.7: Effect of consistency on pulp brightness [1].

1.4.4 Time and temperature

Time and temperature are the most closely related variables affecting the brightness response of mechanical pulp. An increase in bleaching temperature can compensate for a reduction in the retention time up to a point. When TMP is bleached at different temperatures under optimized total alkalinity, two effects are apparent, as illustrated in figure 1.8.

1. At higher temperatures, brightness development is rapid, reaching a maximum in 30 minutes or less.

2. Although brightness development is more rapid at higher temperatures, final brightness is less than that achieved with the same chemical charge at lower temperature.

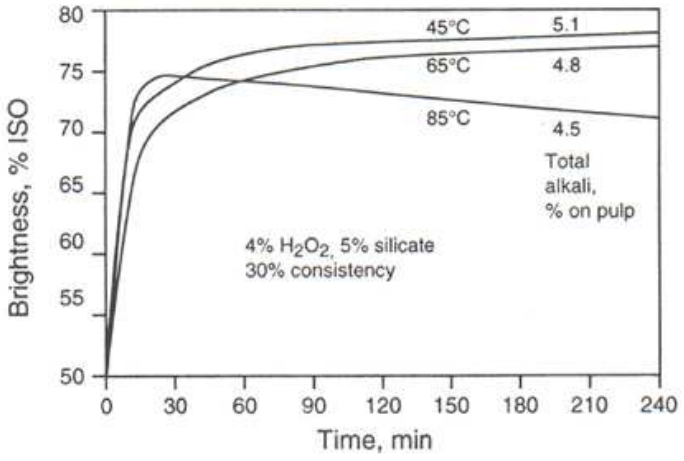

Figure 1.8: The effect of temperature on the rate of brightness development [1].

The rapid decrease in brightness observed for the high temperature ($85°C$ and above) bleach is a result of the peroxide being totally consumed. This occurs because, at high temperatures, the reaction rates of both the bleaching and the decomposition reactions are increased. The retention required for full brightness development may be on the order of two or more hours at $60° - 70°C$. A detailed discussion of all the parameters which affect the mechanical pulp bleaching process, has been presented in this chapter. So that any process control engineer who is interested in controlling the bleaching process, will have a clear and detailed picture of the bleaching process in terms of its process variables.

Chapter 2

The Identification of Mechanical Pulp Bleaching Dynamics

2.1 Introduction

Peroxide bleaching is today mostly manually controlled. The charges of bleaching chemical are regulated principally by taking into consideration the production of pulp and the desired final brightness. When a change in brightness occurs as a consequence of disturbance such an altered pulp consistency and/or quality of wood, there is a considerable passage of time before detection and before a correction can be made. This can result in a waste of bleaching chemicals and uncontrolled final brightness of the bleached pulp.

To achieve automatic control and optimization of the bleaching process, it is advantagous to transform the elimination of chromophores and all other affecting factors into a mathematical model. Basically there are two ways of constructing the mathematical model of the process [6]:

- Mathematical modelling
- System identification

2.2 Mathematical modelling of the bleaching process

This approach uses the physical and chemical laws that dictate the mechanical pulp bleaching process to describe its dynamic behaviour. Basically these laws can be divided into two categories. The first category mainly involves the chemical kinetics of the bleaching reaction itself, the other handles the dynamics of the pulp transport and mixing in the continuous flow system, which mainly consists of the bleaching tower, pipes, and storage tanks.

The bleaching reaction reduces the chromophores concentration, which are the main color-contributing elements in the pulp. The kinetic model of the bleaching reaction can be represented by the Moldenius' empirical model [7],

$$-\frac{dC_k}{dt} = K_r[H_2O_2]^{0.67}[OH^-]^{0.23}{C_k}^{2.2} \tag{2.1}$$

where C_k is the chromophores concentration, K_r is the reaction constant, $[H_2O_2]$ is the peroxide concentration, and $[OH^-]$ is the alkaline ion concentration.

Kinetic analysis has shown that peroxide bleaching has little effect on the light scattering coefficient of the pulp, S. In fact, the peroxide bleaching reaction only

affects the light absorption coefficient of the pulp, K, which is directly proportional to the chromophores concentration [7],

$$K = \alpha C_k \tag{2.2}$$

where α is a constant. The Kulbelka-Munk equation defines the relationship between the pulp brightness B and its light coefficients K and S [3].

$$\frac{B}{100} = 1 + \frac{K}{S} - \sqrt{2(\frac{K}{S}) + (\frac{K}{S})^2} \tag{2.3}$$

The bleaching tower is the main contributing element in the continuous flow system of the bleaching process. In order to model the dynamics of the bleaching tower, it is necessary to know the flow pattern of the pulp stock inside the tower. The flow pattern not only determines the residence time distribution of the reacting materials, but also controls the effectiveness of the bleaching process itself.

The pulp stock is virtually in a state of plug flow inside the tower. The bleaching tower can therefore be represented by a continuous stirred tank reactor *CSTR* followed by a plug flow reactor *PFR*. Consequently the mathematical model of the tower assuming that the volume of the pulp inside the tower is constant, is given by [8]:

$$\dot{C_{ko}}(t - T_d(t)) = -\frac{Q(t)}{V_{CSTR}} C_{ko}(t - T_d(t)) + \frac{Q(t)}{V_{CSTR}} C_{ki}(t) \tag{2.4}$$

where C_{ki}, C_{ko} are the chromophores concentrations at the tower inlet and outlet respectively, $Q(t)$ is the pulp flow, V_{CSTR} is the volume of the mixing part of the tower, and T_d is the delay time resulted from the pulp travel inside the plug flow part of the tower.

Simulation studies [9] on the mathematical model given by equations 2.1, 2.2, 2.3, and 2.4, have shown that the bleaching process can be modelled by first order nonlinear dynamics plus a delay time. The peroxide dosage may be treated as the model input, and incoming pulp brightness and consistancy can be considered as measured disturbances.

2.3 System identification of the bleaching process

System identification is performed by exciting the process and observing its input and output over a time interval. Then a parametric model of the process is fitted to

the recorded input and output sequence. This involves choosing a model structure and a fitting criterion. Once the parameters are estimated, the model is validated to see if it is an appropriate representation of the process. If not, then a more complex model structure must be considered. The estimation of the model structure and parameters is done iteratively in practice [6].

The prediction error method is one of the primary approaches for system identification. It minimizes the prediction error of the process model, and has the advantage of being applicable for all model structures as illustrated in figure 2.1. The fitting criterion $V_N(\theta, Z^N)$ can be expressed in terms of the model parameters θ, the data set with N samples Z^N, and any function of the prediction error $l(\epsilon(t,\theta))$ as [10]:

$$V_N(\theta, Z^N) = \frac{1}{N}\sum_{i=1}^{N} l(\epsilon(t,\theta)) \quad \hat{\theta}_N = \arg\min_{\theta} V_N(\theta, Z^N) \tag{2.5}$$

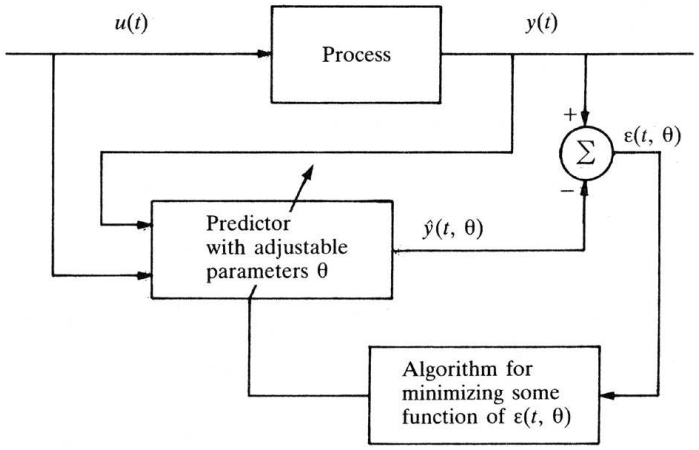

Figure 2.1: Block diagram of the prediction error method.

2.4 Practical aspects

Since the bleaching process is complex and time-varying, neither mathematical modelling nor standard system identification methods can be applied alone. Besides, if linear time-invariant models are used in the identification procedure, the time variability of the flow system will result in inaccurate linear time-invariant models with unacceptably high variance of the parameters estimated [11].

It often happens that a model structure with a number of unknown parameters can be derived from physical laws in most real-world processes such as the bleaching process at Irving Paper mill. Identification methods can then be applied to estimate the unknown parameters.

Data records form Irving Paper mill as well as the bleaching process flowsheet, as indicated in figure 2.2, have shown that the bleaching process model can be intepreted as three separate dynamics [12] [2]:

- A pure gain K represents the bleaching reaction kinetics, since the reaction location is far from the brightness sensor.
- A long variable delay time T_d results from the plug flow pattern of the bleaching tower.
- A first order dynamics with a time constant τ due to the SO_2 mixing process at the bottom of the tower.

In order to estimate the parameters of the bleaching process at Irving Paper mill, a two-stage procedure has to be applied. The variable delay time is estimated in the first stage, and in the second one the other process parameters are estimated.

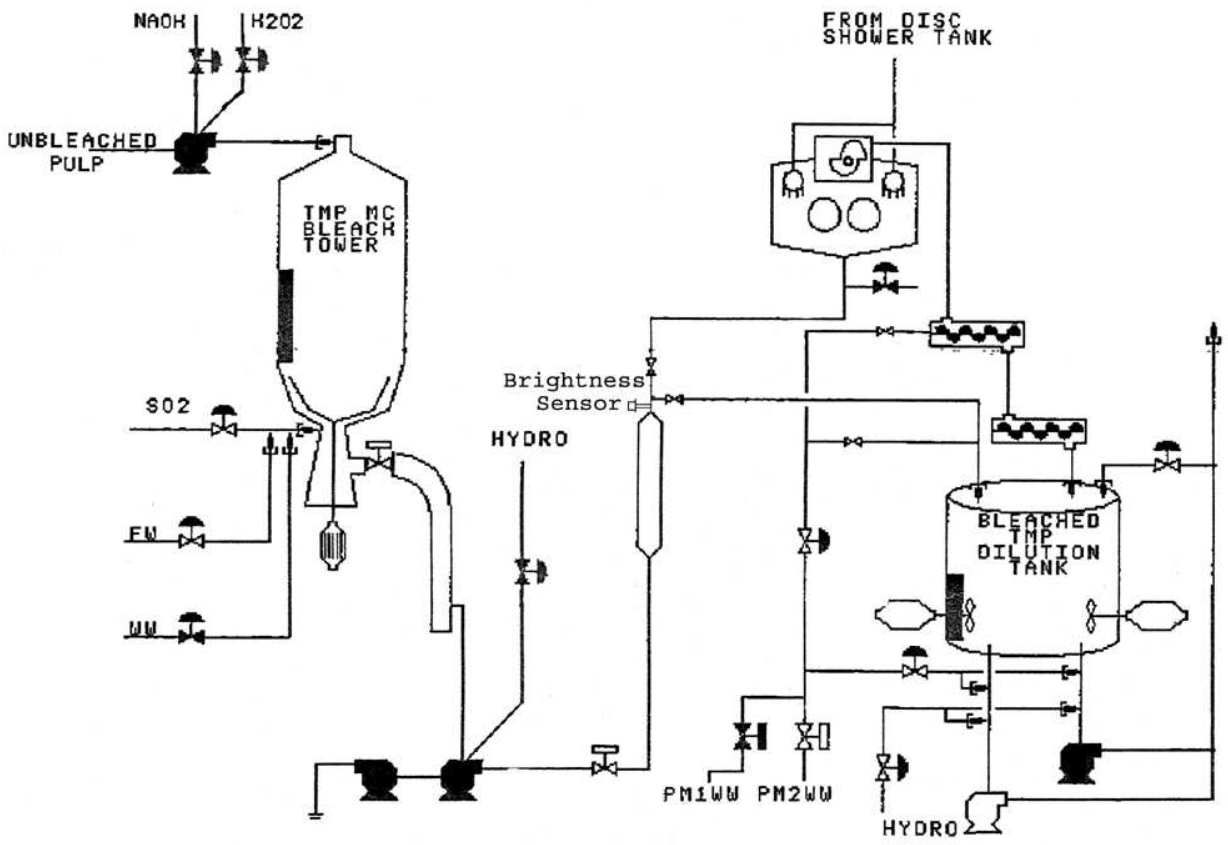

Figure 2.2: Flowsheet of the Bleaching process at Irving Paper [2].

2.4.1 Delay time estimation

The material tranport in a plug flow reactor can be modelled by a delay time. If the flow rate is not constant, the delay time becomes time-varying, which causes difficulty in the analysis and simulation of the process. The traditional theory characterizes the flow of material in a chemical reactor by using concepts like residence time distribution, step response, and intensity functions. A new idea, the volumetric time scale, has been derived form these concepts to estimate the delay time.

The volumetric time scale introduces a new transformation of the time scale, which makes the process model time-invariant even though the flow rate is contiuously varying. It has been used in the application of control engineering because it allows the use of classical time-invariant design methods [11, 13, 14]. If the volume of the material inside the reactor is variable, the volumetric time scale is not applicable.

Zenger et al [15] introduced the concept of a variable delay function, which can be used to estimate the delay time even though the volume is varying. The definition of the delay function has been derived from the theoretical definition of plug flow in a vessel. During the time that a hypothetical concentration pulse stays in the vessel, the volume of material must pass through the vessel irrespective of the flow changes. This can be stated mathematically as:

$$\int_{t-Td(t)}^{t} Q_{out}(\tau)d\tau = V(t - T_d(t)) \tag{2.6}$$

where t is the time at which the material exits the reactor, Q_{out} is the outflow, and T_d is the transport delay. Alternatively, the delay function can be expressed in terms of inflow Q_{in} by substituting $\dot{V}(t) = Q_{in}(t) - Q_{out}(t)$ in equation 2.6:

$$\int_{t-Td(t)}^{t} Q_{in}(\tau)d\tau = V(t) \tag{2.7}$$

An algorithm for time delay estimation can be developed by using either equation 2.6 or 2.7 as follows:

1. Store the inflow measurements over a time interval which equals the maximum retention time of the reactor, with sampling time h.

2. Measure the volume at time t and set the counter $k = t - h$.

3. Intergrate the inflow backwards from k to t.

4. If the integration result equals the volume at time t then stop and $T_d(t) = t-k$.

5. Else set $k = k - h$ and goto step 3.

This algorithm can be used for both identification and control purposes.

2.4.2 Model parameter estimation

Once the delay time sequence has been estimated for a certain data set, a least square fitting procedure is then applied to estimate the model parameters (i.e., gain and time constant). The bleaching process at Irving Paper is manually controlled by changing the peroxide dosage depending on both the incoming and the target pulp brightnesses, whereas the other process variables are kept constant. The two-stage identification procedure has been implemented on two real different data sets in order to examine its reliability.

Simulation results have shown that the gain of the process is nonlinear and dependent on the peroxide dosage. The time constant of the bleaching process is in the vicinity of 50 minutes. This is unobservable, due to the long residence time in the reactor. Figures 2.3 and 2.5 show the the estimated delay time from the pulp inflow and volume for the two data sets. The delay time estimation algorithm seems to have worked well, because the transient parts of both the estimated and the real brightness reponses take place nearly at the same time for the two data sets as illustrated in figures 2.4 and 2.6. The results are not entirely accurate, because of the noisy data, ignorance of the incoming pulp brightness, and the existence of disturbances.

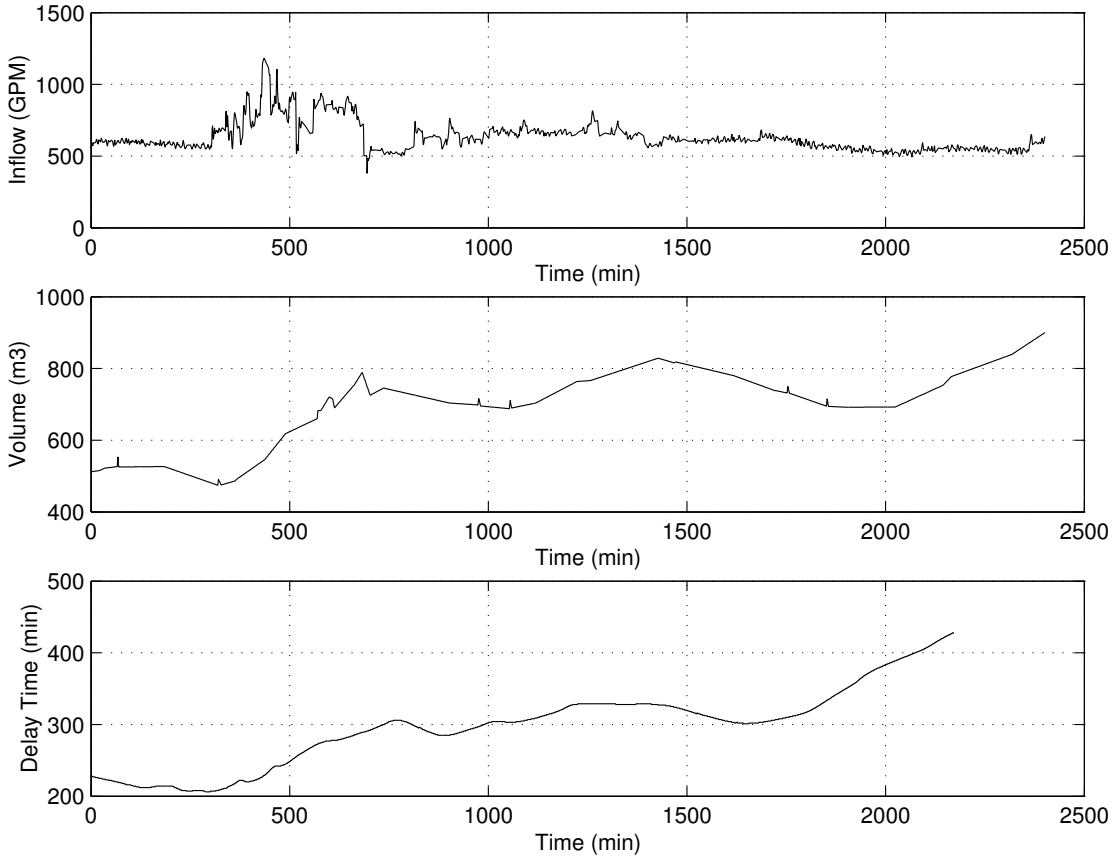

Figure 2.3: The estimated delay time, first data set.

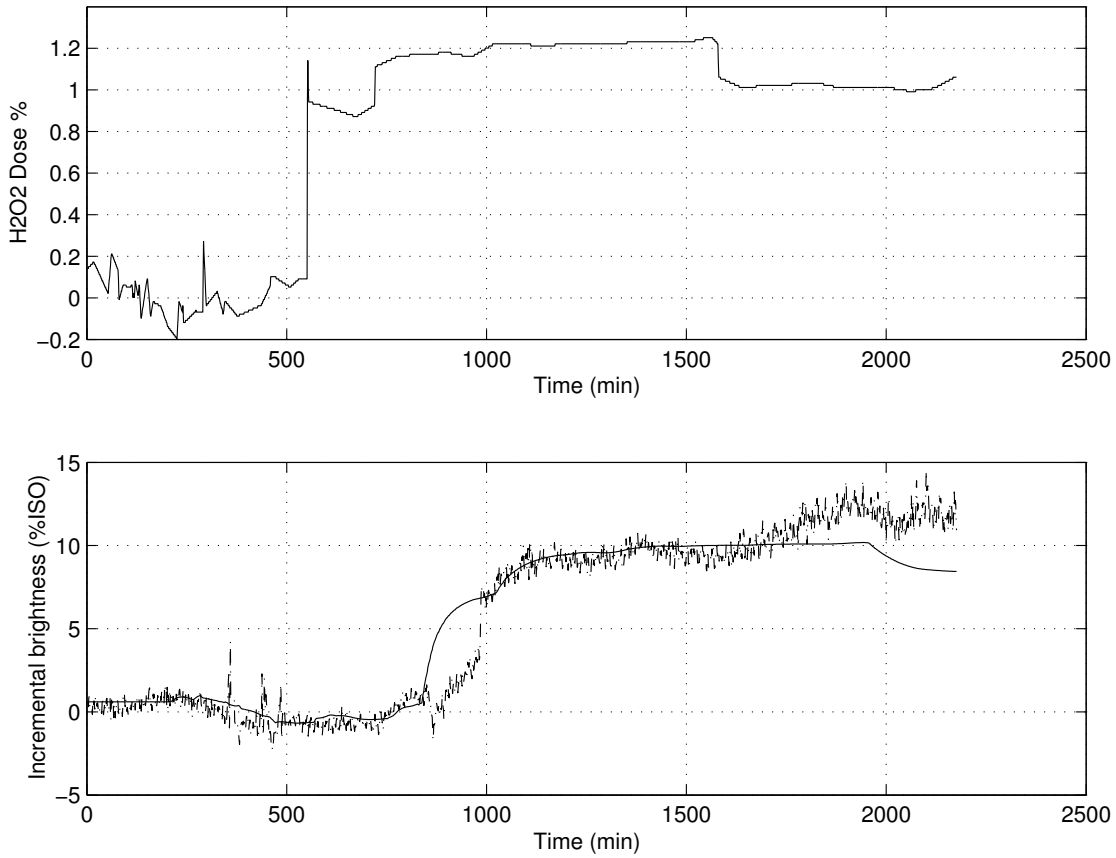

Figure 2.4: The estimated and real pulp brightness, first data set.

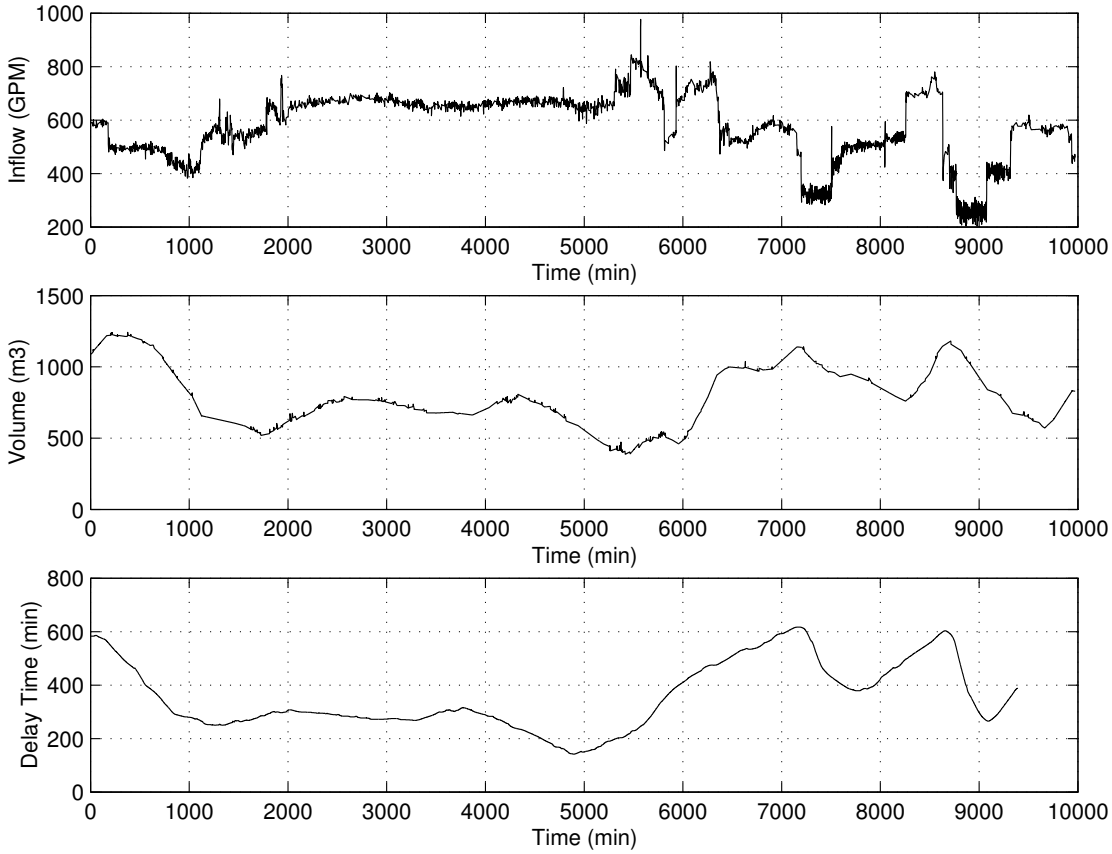

Figure 2.5: The estimated delay time, second data set.

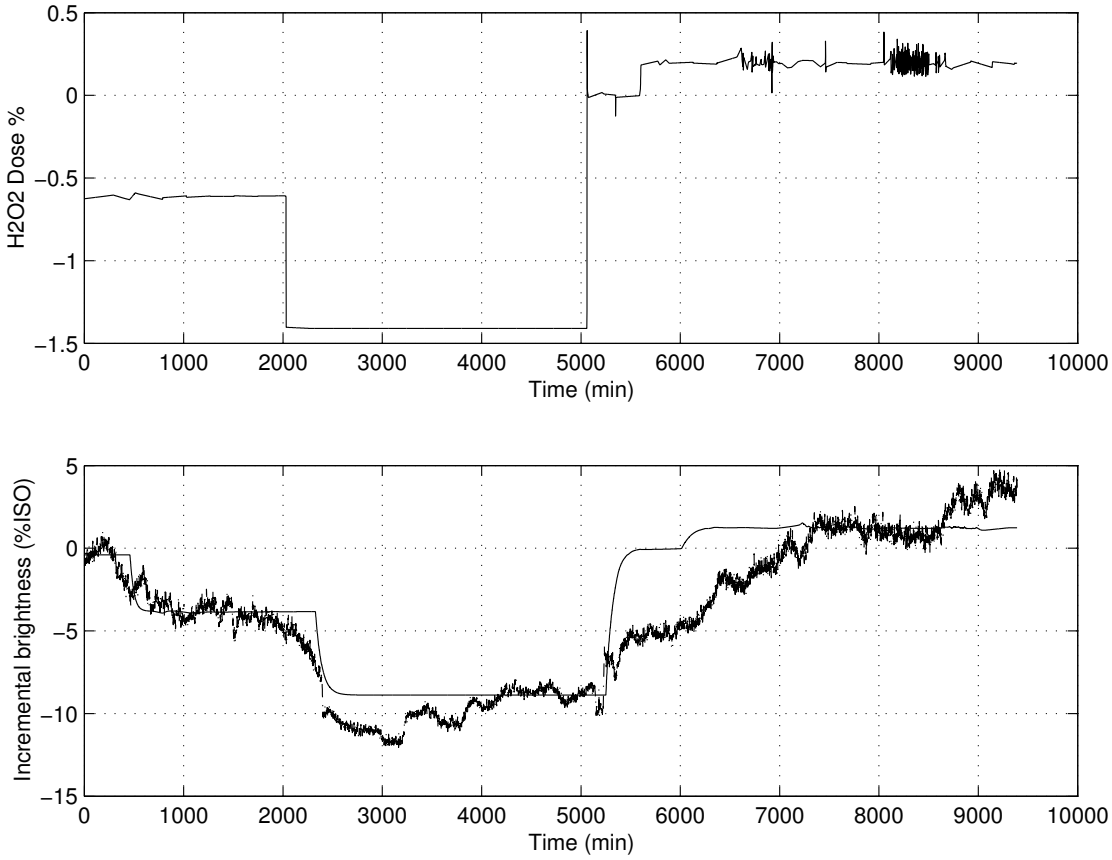

Figure 2.6: The estimated and real pulp brightness, second data set.

2.5 The SO_2 effect on the brightness response

Sulphur dioxide is added to the pulp at the end of the bleaching process to destroy the peroxide residual and to reduce the pH of the pulp to around $4-5$. The SO_2 mixing process is done at the bottom of the bleaching tower at Irving Paper mill. Data records and simulation results have shown that SO_2 has a significant effect on the final brightness response [12, 2]. This effect can be summerized by two observations as illustrated in figure 2.7, where the SO_2 dosage plot has been scaled by a factor of 8 to have the same scale as the brightness plot magnitude:

1. Secondary dynamics with a smaller time constant compared to the mixing process time constant, dominate the brightness response as SO_2 is added to the pulp at $t \cong 1000$ min.

2. Any disturbance in the SO_2 dosage will result in an exact corresponding disturbance in the brightness response, as happens at $t \cong 1700$ min. This has been verified by running the identification procedure on the bleaching process with two inputs, where the second input was the SO_2 dosage. The simulated brightness closely matches the actual one.

The alkalinity level at the top of the bleaching tower where the bleaching reaction takes place, is not controlled at all. This implies that any increase in the alkalinity level, for any reason, would result in a higher brightness gain. On the other hand, it also means that more SO_2 has to be added to compensate for the higher level of pulp PH, which in turn causes a disturbance in the final brightness response. This explains the second effect of SO_2 on pulp brightness response.

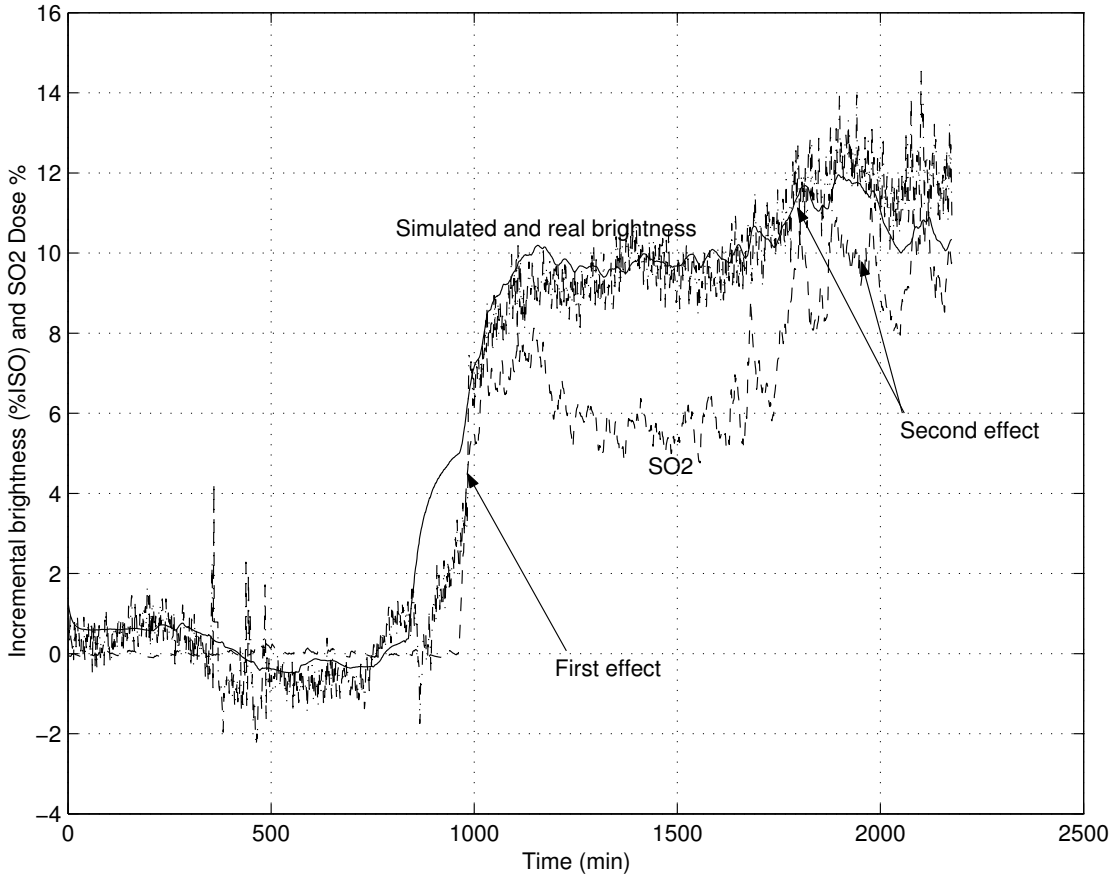

Figure 2.7: The SO_2 effect on pulp brightness.

Chapter 3

Controller Design

3.1 Model predictive control

Model predictive control (*MPC*) originated in the late seventies and has developed considerably since then. Several studies contributed to the developement of the *MPC* stategy including model algorithmic control (*MAC*) of Richalet in 1978, dynamic matrix control (*DMC*) of Cutler and Ramaker in 1979 [16], and generalized predictive control (*GPC*) of Clarke in 1987 [17].

The objectives behind the development of these strategies were very different. *DMC* and similar strategies were conceived to tackle the multivariable constrained problems typical for oil and chemical industries. However, the *GPC* strategy was intended to offer a new adaptive control alternative. The traditional transfer function model was employed in *GPC*. While the *DMC* formulation was completely deterministic, stochastic aspects played a key role in *GPC* [18]. One may refer to many survey papers to get a better idea about the history of the MPC control strategy such as Qin and Badgwell 1997 [19], and Morari and Lee 1999 [18].

The *MPC* strategy presents many strengths that make it more attractive than the classical *PID* controller. Among the strengths which stand out:

- It can be used to control a great variety of processes, including systems with long delay times, non minimum phase response, and instability.
- It intrinsincally has compensation for dead times.
- It introduces feed-forward control in a natural way to compensate for measurable disturbances.
- Its extension to the treatment of constraints is conceptually simple.
- The multivariable case can easily be dealt with.
- It is very useful when future reference trajectories are known, in cases such as robotics and batch processes.

There are many successful applications of the *MPC* strategy in use, not only in the process industry but also in the other industries. Mechanical pulp bleaching process is a very challenging application, which is going to be controlled by using the *MPC* strategy in this thesis.

3.2 Dynamic matrix control

MPC is an optimal control strategy that uses a plant model to predict the effect of an input profile on the evolving state of the plant. At each sampling instant, an optimal control problem is solved and its optimal plant input profile is implemented until another measurement becomes available. The updated plant information is used to formulate and solve a new optimal control problem, and the process is repeated. This strategy yields a receding horizon control problem [20]. Dynamic matrix control *DMC* is the particular *MPC* method which is going to be analyzed and used to control the bleaching process due to its simplicity and efficiency.

3.2.1 Prediction

The process model employed in the *DMC* formulation is the step response of the plant, while the disturbance is considered to keep constant along the horizon. The procedure to obtain the prediction is as follows [20]: The discrete-time response model of the plant is $y(t) = \sum_{i=1}^{\infty} g_i \Delta u(t-i)$ where g_i are the sampled output values for the step input and $\Delta u(t) = u(t) - u(t-1)$ is the input increment, so the prediction values along the horizon will be:

$$\hat{y}(t+k|t) = \sum_{i=1}^{\infty} g_i \Delta u(t+k-i) + \hat{n}(t+k|t) \tag{3.1}$$

$$= \sum_{i=1}^{k} g_i \Delta u(t+k-i) + \sum_{i=k+1}^{\infty} g_i \Delta u(t+k-i) + \hat{n}(t+k|t) \tag{3.2}$$

Disturbances are considered to be constant $\hat{n}(t+k|t) = \hat{n}(t|t) = y_m(t) - \hat{y}(t|t)$, where y_m is the measured output. This leads to:

$$\hat{y}(t+k|t) = \sum_{i=1}^{k} g_i \Delta u(t+k-i) + \sum_{i=k+1}^{\infty} g_i \Delta u(t+k-i) + y_m(t) - \sum_{i=1}^{\infty} g_i \Delta u(t-i) \tag{3.3}$$

The prediction of the output sequence can be separated into two parts [20]. One of them , the free response, corresponds to the evolution of the present state of the process due to the past control moves. The other part, the forced response, is due to the future control moves, as illustrated in figure 3.1.

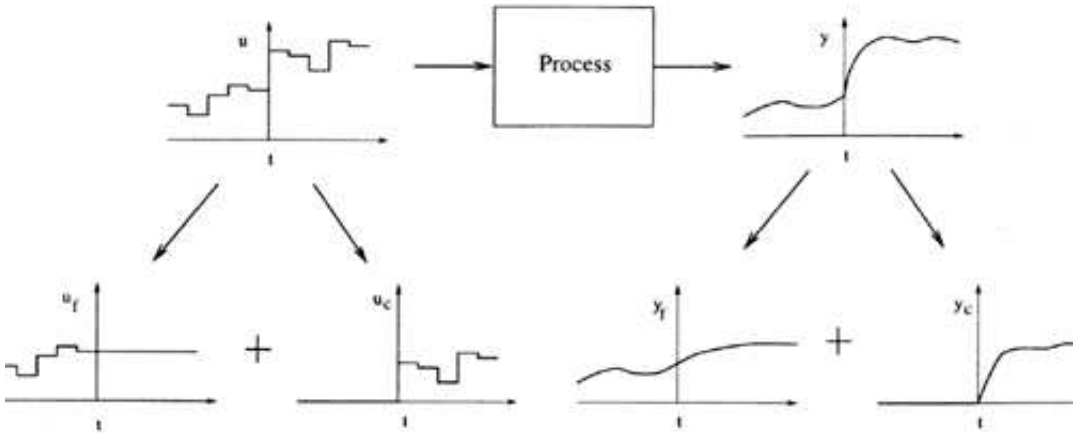

Figure 3.1: Forced and free response.

The prediction can then be expressed as:

$$\hat{y}(t+k|t) = \sum_{i=1}^{k} g_i \Delta u(t+k-i) + f(t+k|t) \tag{3.4}$$

$$f(t+k|t) = y_m - \sum_{i=1}^{\infty} (g_{k+i} - g_i)\Delta u(t-i) \tag{3.5}$$

where $f(t+k|t)$ is the free response. If the process is asymptotically stable, the coefficients g_i of the response model tend to be constant after N_P sampling periods, which implies that $g_{i+k} - g_i \approx 0$ for $i > N_P$. Therefore, the free response can be approximated as:

$$f(t+k|t) = y_m - \sum_{i=1}^{N_P} (g_{k+i} - g_i)\Delta u(t-i) \tag{3.6}$$

Now the prediction can be computed along the prediction horizon N_P, considering N_U control actions:

$$\hat{y}(t+1|t) = g_1 \Delta u(t) + f(t+1|t) \tag{3.7a}$$

$$\hat{y}(t+2|t) = g_2 \Delta u(t) + g_1 \Delta u(t+1) + f(t+2|t) \tag{3.7b}$$

$$\vdots \tag{3.7c}$$

$$\hat{y}(t+N_P|t) = \sum_{i=1}^{N_P} g_i \Delta u(t+N_P-i) + f(t+N_P|t) \tag{3.7d}$$

hence the prediction can be expressed in terms of the system's dynamic matrix G,

the control increments vector U, and the free response vector F as:

$$\hat{Y} = GU + F \tag{3.8}$$

where G is made up of N_U columns of the system's step response appropriately shifted down in order.

$$G = \begin{pmatrix} g_1 & 0 & \dots & 0 \\ g_2 & g_1 & \dots & 0 \\ \vdots & \vdots & \ddots & \vdots \\ g_{N_U} & g_{N_U-1} & \cdots & g_1 \\ \vdots & \vdots & \ddots & \vdots \\ g_{N_P} & g_{N_P-1} & \cdots & g_{N_P-N_U-1} \end{pmatrix}$$

3.2.2 Measurable disturbances

Measurable disturbances can easily be added to the prediction equations, since they can be treated as inputs. Equation 3.8 can be used to calculate the predicted disturbances,

$$\hat{Y}_d = Dd + F_d$$

where $\hat{Y}_d$ is the contribution of the measurable disturbance to the system output, D is a matrix containing the coefficients of the sysem response to a step in the disturbance, d is the vector of disturbance increments, and F_d is the part of the response that does not depend on the disturbance.

The complete free response of the system can be considered as the sum of two effects: the response to the past input F_U and to the measurable disturbance effect $F = F_U + Dd + F_d$. Therefore the prediction can be computed by the general expression given previously by equation 3.8.

3.2.3 Objective function

The objective of a *DMC* controller is to drive the future output sequence $\hat{Y}$ as close to a specified future reference trajectory $W = \{w(t+1), w(t+2), \cdots, w(t+N_p)\}$ as possible in a least square sense, with the possibility of the inclusion of a penalty term on the input moves. Specifically, the manipulated variables are selected to minimize a quadratic objective based on the future errors and the control effort:

$$J = \sum_{j=1}^{N_P} [\hat{y}(t+j|t) - w(t+j)]^2 + \sum_{j=1}^{N_u} \lambda [\Delta u(t+j-1)]^2 \tag{3.9}$$

where λ is a positive constant that can be used to tune the *DMC* controller to meet the required performance. The cost function can be expressed in terms of the future error along the prediction horizon $e = \hat{Y} - W$ and the future control sequence U as $J = e^T e + \lambda U^T U$.

3.2.4 Reference trajectory

The future evolution of the reference $r(t+k)$ is known beforehand in many applications such as robotics, servos, or batch processes. The *DMC* method usually uses a reference trajectory $w(t+k)$, which does not necessarily have to coincide with the real reference $r(t+k)$. It is normally a smooth approximation from the current value of the output $y(t)$ towards the known reference $r(t)$ by means of the first order system,

$$w(t) = y(t), \;\; w(t+k) = \alpha w(t+k-1) + (1-\alpha) r(t) \;\; k = 1 \ldots N_P$$

where the parameter $0 \leq \alpha \leq 1$ constitutes an adjustable value that will influence the system's dynamic response. The closer the value of α to 1 the smoother the approximation, as illustrated in figure 3.2.

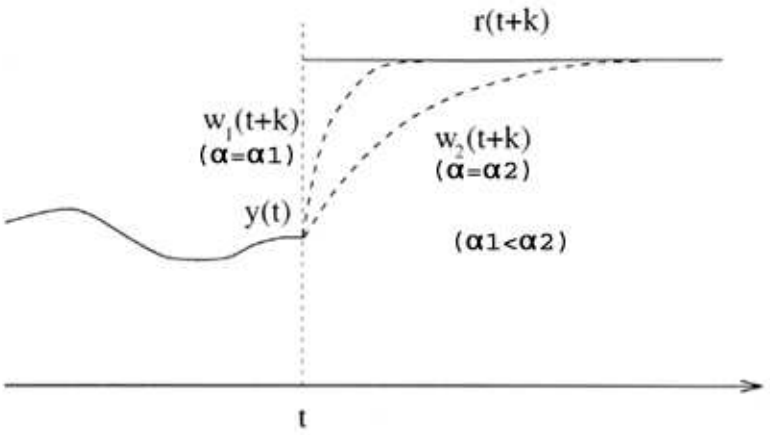

Figure 3.2: Reference trajectory.

3.2.5 The unconstrained *DMC* case

In order to obtain the optimal input profile, it is necessary to minmize the cost function 3.9. The number of variables in the optimization problem can be reduced

significantly by introducing the control horizon concept, which considers that after a certain interval $N_U < N_P$ there is no variation in the proposed control signal.

$$\Delta u(t+j-1) = 0 \;\; for \;\; j > N_U$$

The future control increments can be obtained analytically for this case by computing the derivative of the cost function 3.9 and making it equal to 0. This leads to the optimal input profile:

$$U = (G^T G + \lambda I)^{-1} G^T (W - F) \tag{3.10}$$

3.2.6 The constrained *DMC* case

In real world applications, all processes are subject to constraints. Actuators have a limited range of action and a limited slew rate. Safety reasons as well as sensor range cause bounds in process variables. Furthermore, the operating points of a plant are determined to satisfy economic goals and lie at the intersection of certain constraints.

The constraints acting on a $SISO$ process over a over a receding horizon N_U, originate from amplitude limits in the control signal, slew rate of the actuator, and limits on the output signal. They can be expressed in terms of the control increments vector U as:

$$u_{min} l \leq \; TU + u(t-1)l \; \leq u_{max} l \tag{3.11a}$$

$$du_{min} l \leq \; U \; \leq du_{max} l \tag{3.11b}$$

$$y_{min} l \leq \; GU + F \; \leq y_{max} l \tag{3.11c}$$

where l is an $N_U \times 1$ vector whose all elements are ones, and T is an $N_U \times N_U$ lower triangular matrix whose non null entries are ones. The constraints can be expressed in a condensed form as [20]:

$$RU \; \leq \; C \tag{3.12}$$

where

$$R = \begin{bmatrix} I_{N_U \times N_U} \\ -I_{N_U \times N_U} \\ T \\ -T \\ G \\ -G \end{bmatrix} \quad C = \begin{bmatrix} du_{max} l \\ -du_{min} l \\ u_{max} l - u(t-1)l \\ -u_{min} l + u(t-1)l \\ y_{max} l - F \\ -y_{min} l + F \end{bmatrix}$$

The cost function of the *DMC* strategy is quadratic and can be rewritten in terms of the control increments by substituting equation 3.8 in equation 3.9 as:

$$J(U) = \frac{1}{2}U^T HU + b^T U + c \tag{3.13}$$

where $H = 2(G^T G + \lambda I)$ is the hessian of $J(U)$, $b^T = 2(F - W)^T G$ is a $1 \times N_U$ vector, and $c = (F - W)^T (F - W)$ is a constant.

It is easy to show that the *DMC* optimal control problem is a convex quadratic programming problem since:

- The cost function is quadratic with a positive definite hessian, which results in a convex cost function.
- The constraints are linear inequalities which comprise a convex set.

In order to solve the optimal control problem imposed by the constrained *DMC* strategy, numerical optimization algorithms have to be implemented. They are discussed in the next chapter.

3.3 The effect of penalizing the control moves

Structuring the control law in the *DMC* controller produces an improvement in robustness and in the general behaviour of the system. This is done by introducing the principle of a finite control horizon and adding a penalty term on the control moves to the objective function. However, allowing the free evolution of the control signal without being structured may lead to undesirable high frequency control signals and, in the worst case, to instability [20].

A first order system controlled by the *DMC* strategy was simulated to study the effect of penalizing the control moves on the system response. The simulation has addressed both the unconstrained and the constrained cases and the control horizon was chosen fairly large, $N_U = 20$. Penalizing the control moves has a great impact on the system performance, as the simulation has shown. The system became unstable in the absence of the control penalty term in the objective function, as illustrated in figure 3.3, which is clear from the large control signal in the optimal input profile (top trace). However the system becomes stable and its

performance is considerably improved in the presence of the control penalty term for the unconstrained case (middle & bottom traces).

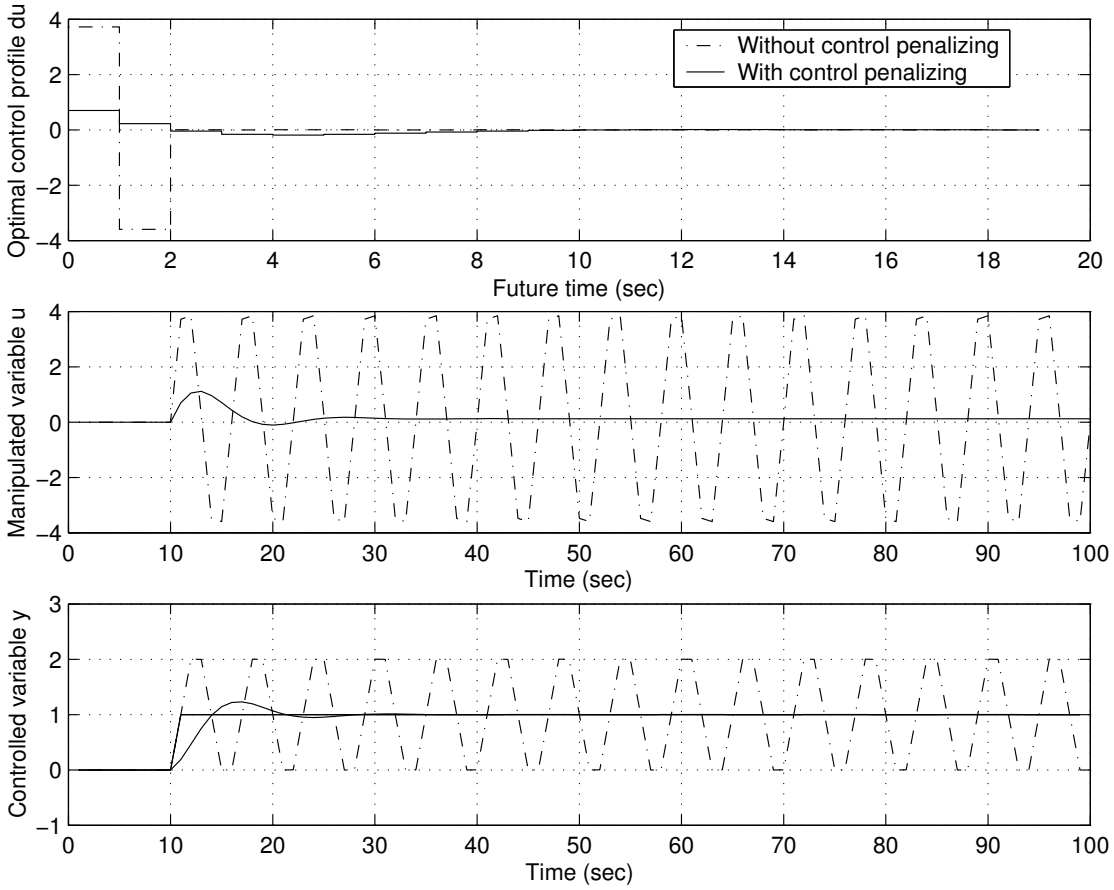

Figure 3.3: The effect of structuring the control law for the unconstrained case.

The system performance seems to be better in the presence of constraints even though the control moves are not penalized, as the simulations have shown. But when a comparison between the system responses with and without structuring the control law is made in the presence of input constraints U as illustrated in figure 3.4, the system has shown a better response when the control law was structured. Simulations have shown that structuring the control law is a necessity regardless of the presence of constraints.

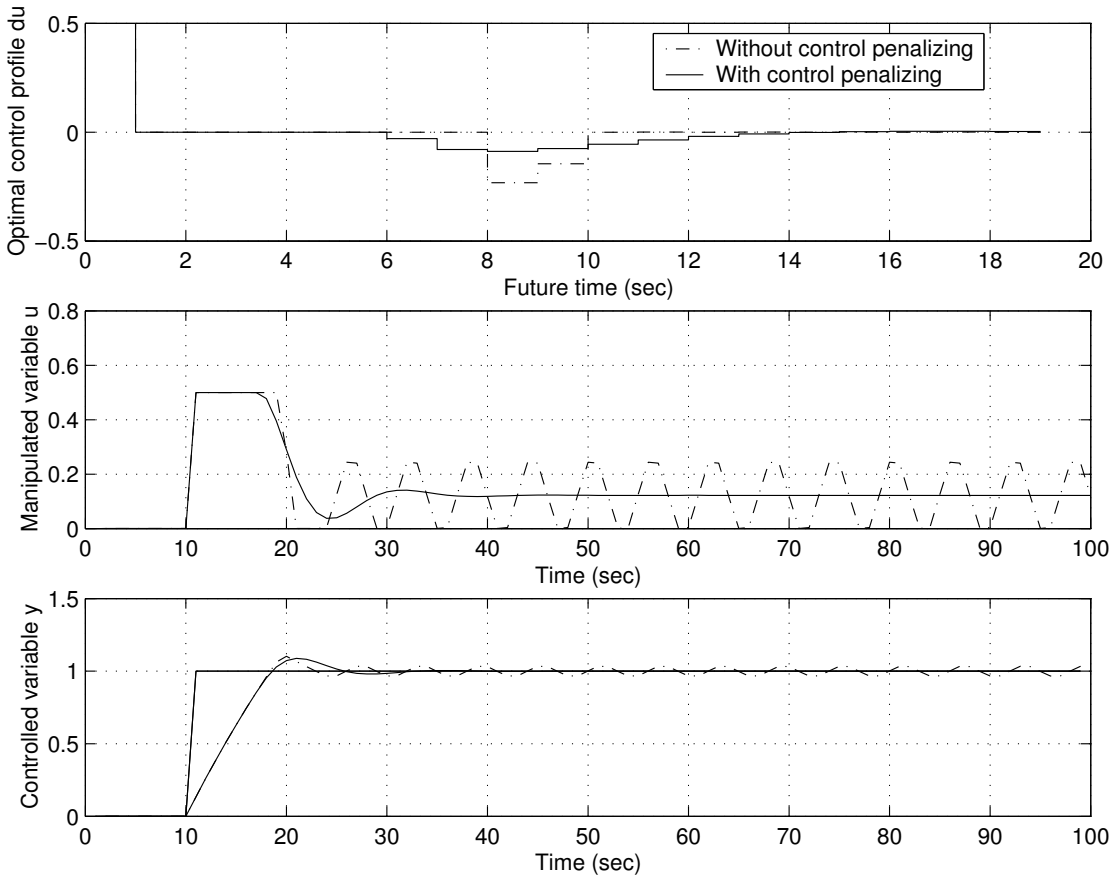

Figure 3.4: The effect of structuring the control law for the constrained case.

3.4 *DMC* strategy for variable delay-time systems

A plant with delay-free part $G(s)$ and a series delay T_d represented by $G(s)e^{-sT_d}$ can be controlled effectively by delay free methods if a series controller could cancel the delay term. Predictive control methods are techniques in which a predictor is included to cancel the delay term of the plant. Smith predictor and model predictive control *MPC* are examples of such techniques.

In order for the *DMC* strategy to handle systems with constant delay time, the prediction horizon N_P should be extended to include the delay time T_d. This implies that the first T_d rows of the dynamic matrix G should be zeros, to capture the delay time. The *DMC* strategy can also handle variable delay time $T_d(t)$ if the delay time is accurately estimated at each sampling instant, so that the dynamic matrix G includes the right number of zero rows at its top at each sampling instant.

A first order system with variable delay time controlled by the *DMC* strategy, is simulated to study the effect of variable delay time on the system performance. Two approaches were tested; in the first one the same variable delay time function acting on the plant was applied to the *DMC* controller, and a constant delay time was applied to the controller in the second approach. As illustrated in figure 3.5, the system responded differently in the two cases when it was excited by a train of unit pulses occuring at different levels of the variable delay time function (top trace). The system showed a better performance (middle and bottom trace) for the first approach (solid line) rather than the constant delay time approach (dash-dotted line). Simulations have shown that variable delay time systems do require that the same variable delay time acting on the plant should be applied to the *DMC* controller.

The prediction in predictive control techniques depends on how well the plant is modelled. The performance in such techniques is sensitive to the differences between the actual parameters of the plant and its model. The effects of these differences between a plant and its model are called mismatch problems. Temporal mismatch is the difference between the actual delay and its nominal value, whereas parametric mismatch denotes to the difference between the delay-free part of a plant and its model. Several research studies have addressed the importance of mismatch problems where a high performance predictive controller is required. They have indicated that temporal mismatch poses the biggest challenge to both performance and stability of variable delay time systems [21, 22, 23].

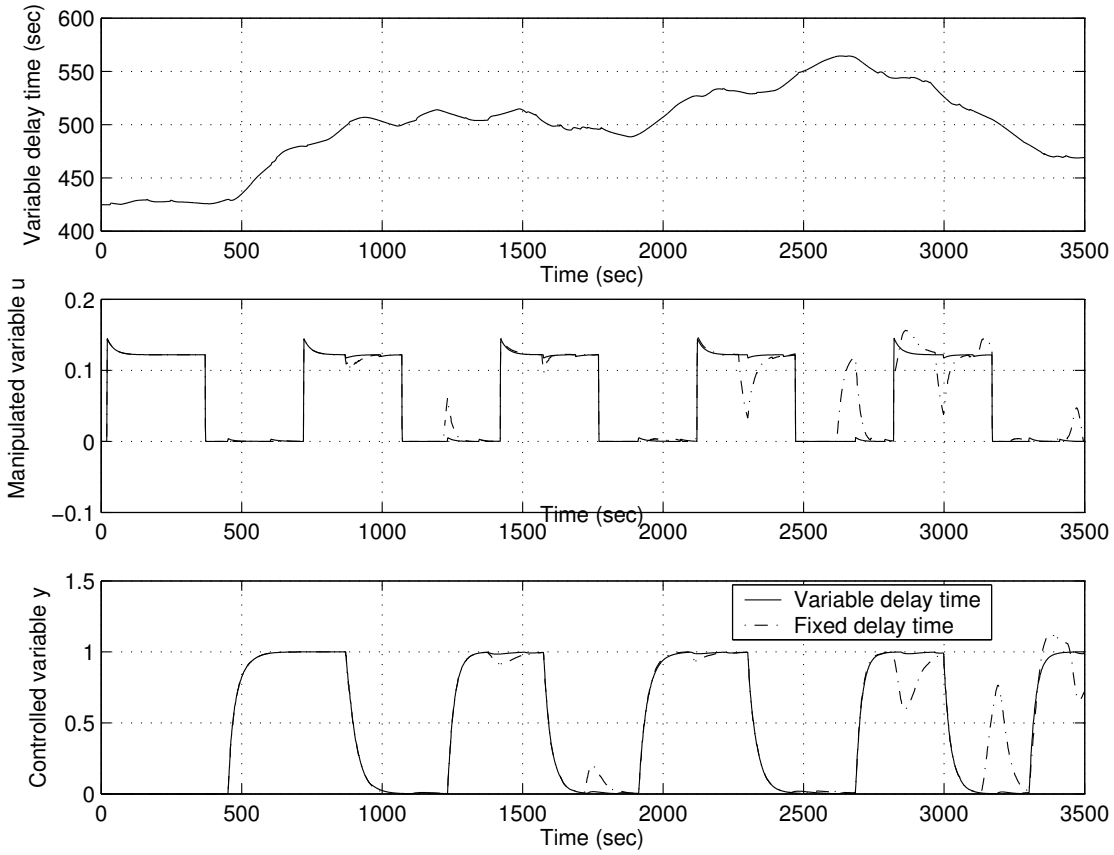

Figure 3.5: Comparison between variable and constant delay time DMC controllers.

Chapter 4

Optimization Algorithms For Convex Quadratic Programming

4.1 Introduction

It has been shown in the previous chapter that the optimal control problem imposed by the *DMC* controller of the bleaching process is a convex quadratic programming (QP) problem. The QP problem represents a special class of nonlinear programming, in which the objective function is quadratic and the constraints are linear. There are several classes of algorithms for solving the QP problem.

One class is comprised of the penalty and the barrier function methods such as the augumented lagrangian method. In this class the constrained problem is transformed to a single unconstrained problem or a sequence of unconstrained ones. Another class includes the feasible directions approaches, such as the active set method and the gradient projection method. The active set strategy is a combinatorial approach to iteratively determine the set of binding constraints of optimality. This is done by solving a sequence of constrained equality QP problems. The gradient projection method attempts to accelerate the solution process by allowing rapid changes in the active set. It is efficient when the only constraints in the problem are bounds on the variables [24, 25].

One of the popular schemes for solving a quadratic program is to solve the Karush-Kuhn-Tucker KKT system. The class that follows this scheme includes the complimentary pivoting methods such as Lemke's method, and the interior point methods which are effective for solving large scale convex QP problems [24, 26]. Only the two most popular methods for solving convex QP problems are discussed in this chapter.

4.2 Convex quadratic programming

The convex optimization problem is called a convex quadratic program if the objective function is quadratic with a positive semi definite hessian, and the constraints are linear. A general quadratic program can be expresses in its primal form as:

$$\min_{x} \quad \tfrac{1}{2}x^T Q x + c^T x \tag{4.1a}$$

$$\text{subject to} \quad a_i^T x \leq b_i \;\; i \in \mathcal{I} \tag{4.1b}$$

$$a_i^T x = b_i \;\; i \in \mathcal{E} \tag{4.1c}$$

where $Q = Q^T \geq 0$ is a symetric positive semi definite matrix, and the index sets $\mathcal{I}, \mathcal{E}$ specify the inequality and equality constraints respectively. Figure 4.1 illustrates the minimization of a convex quadratic function over an inequality constraint set that defines a polyhydron.

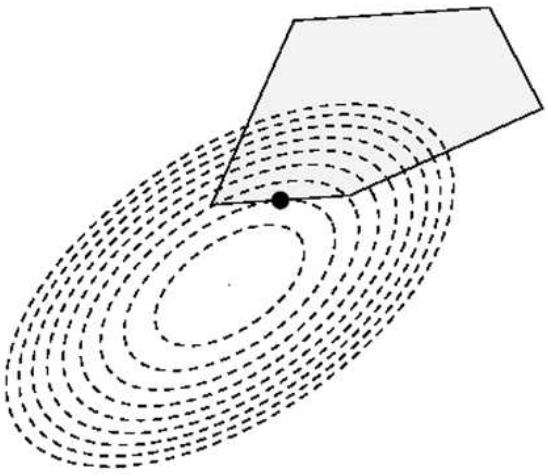

Figure 4.1: Illustration of convex quadratic programming.

The dual of the general QP can be expressed as:

$$\begin{aligned} \max_{x} \quad & -\tfrac{1}{2}x^T Q x - \textstyle\sum_{i\in\mathcal{I}} \lambda_i b_i - \sum_{i\in\mathcal{E}} \lambda_i b_i && \text{(4.2a)} \\ \text{subject to} \quad & Qx + c + \sum_{i\in\mathcal{I}} a_i^T \lambda_i + \sum_{i\in\mathcal{E}} a_i^T \lambda_i = 0 && \text{(4.2b)} \\ & \lambda_i \geq 0 \text{ for } i \in \mathcal{I} && \text{(4.2c)} \end{aligned}$$

where λ_i is the lagrange multiplier for the equality and inequality constraints. Since the QP problem is convex, the KKT conditions become the necessary and sufficient conditions for optimality. The KKT conditions can be expressed as:

$$\begin{aligned} Qx + c + \sum_{i\in\mathcal{I}} a_i^T \lambda_i + \sum_{i\in\mathcal{E}} a_i^T \lambda_i = 0 && \text{(4.3a)} \\ a_i^T x_i - b_i + s_i = 0 \quad i \in \mathcal{I} && \text{(4.3b)} \\ a_i^T x_i - b_i = 0 \quad i \in \mathcal{E} && \text{(4.3c)} \\ \lambda_i s_i = 0 \quad i \in \mathcal{I} && \text{(4.3d)} \\ (\lambda_i, s_i) > 0 \quad i \in \mathcal{I} && \text{(4.3e)} \end{aligned}$$

where s_i, $i \in \mathcal{I}$, is a slack variable for the i^{th} inequality constraint.

4.3 Active set method for convex QP

Active set methods usually start by computing a feasible initial iterate x_0, and then ensure that all subsequent iterates remain feasible. They find a step from one iterate to the next by solving an equality constrained QP subproblem. First the working set $\mathcal{W}_k$is defined, consisting of all the equality constraints together with the active inequality constraints, all other constraints are temporarily disregarded [26]. Then given an iterate x_k and the working set $\mathcal{W}_k$, if x_k does not minimize the cost function in the QP subproblem defined by the working set, then a direction P_k is computed by solving the QP subproblem. The QP subproblem can be expressed in terms of the direction P_k and the gradient of the cost function $\nabla_k = Qx_k + c$ as:

$$\min_{P_k} \quad \tfrac{1}{2} P_k^T Q P_k + \nabla_k^T P_k \tag{4.4a}$$

$$\text{subject to} \quad a_i^T P_k = 0 \ \text{ for all } i \in \mathcal{W}_k \tag{4.4b}$$

Since the hessian Q is positive semi definite, methods such as the range space and the null space techniques can be used for solving the QP subproblem. In order to decide how far to move along the direction P_k, a step length parameter is chosen to be the largest value in the range $[0, 1]$ for which all the constraints are satisfied. The step length α_k is given by the following definition:

$$\alpha_k \stackrel{def}{=} \min(1, \min_{\substack{i \notin \mathcal{W}_k \\ a_i^T P_k < 0}} \frac{b_i - a_i^T x_k}{a_i^T P_k}) \tag{4.5}$$

The constraints i for which the minimum in equation 4.5 is achieved, are called the blocking constraints. If $\alpha_k < 1$, that is the step along P_k was blocked by some constraints not in $\mathcal{W}_k$, a new working set $\mathcal{W}_{k+1}$, is constructed by adding one of the constraints to $\mathcal{W}_k$. The signs of the lagrange multipliers $\hat{\lambda}_i$ corresponding to the inequality constraints in the working set are examined. If the multipliers are all non negative then x_k is the optimal solution of the original problem. However if any of the multipliers are negative, then the most negative one is removed from the working set and a new QP subproblem is solved. The lagrange mutipliers can

be estimated from the following expression:

$$\sum_{j \in \mathcal{W}_k} a_i \hat{\lambda}_i = g_k = Qx_k + c \tag{4.6}$$

Having given a complete discription of the active set algorithm for convex QP, the algorithm can be summarized as follows:

1. Compute a feasible initial point x_0
2. Set $\mathcal{W}_0$, the subset of the active constraints at x_0
3. For $i = 0, 1, 2, \cdots, M$ (M = maximum number of iterations)
   (a) Solve the QP subproblem in 4.4a to find the direction P_k
   (b) If $P_k = 0$
      i. Compute the lagrange multipliers $\hat{\lambda}_i$ from equation 4.6
      ii. If $\hat{\lambda}_i \geq 0$ for all $i \in \mathcal{W}_k \cap \mathcal{I}$, then stop with solution $x^\star = x_k$
      iii. Else
         A. Set $j = arg \min_{j \in \mathcal{W}_k \cap \mathcal{I}} \hat{\lambda}_j$
         B. Set $x_{k+1} = x_k$
         C. Set $\mathcal{W}_{k+1} = \mathcal{W}_k \backslash \{j\}$
   (c) Else ($P_k \neq 0$)
      i. Compute The step length α_k from equation 4.5
      ii. Set $x_{k+1} = x_k + \alpha_k P_k$
      iii. If $\alpha_k < 1$ (there are blocking constraints), then obtain $\mathcal{W}_{k+1}$ by adding one of the blocking constraints to $\mathcal{W}_k$
      iv. Else set $\mathcal{W}_{k+1} = \mathcal{W}_k$
   (d) If $i = M$ stop with semioptimal solution
4. End (for)

4.4 Interior point methods

Since the presentation of the new polynomial-time algorithm by Karmarker in his landmark paper in 1984, the new field of interior point methods has witnessed

rapid development and expansion. On the theoretical side, subsequent research led to improved computational complexity bounds for LP, convex QP, and other classes of convex programming. On the computational side, high quality software was eventually produced.

Interior point methods can be divided to primal and primal-dual methods. They differ from each other in that the primal-dual framework treats the dual variables explicitly in the problem, rather than as adjuncts to the calculation of the primal iterates as in the primal approach. The primal-dual framework has always been popular because it yielded new algorithms with interesting theoretical properties, formed the basis of the best practical algorithms, and allowed the transparent extentions to convex QP and the linear complementary problem (LCP). Potra and Wright [27] reviewed the history of the development of interior point methods and gave a good survey in their paper.

Primal-dual interior point methods for LP and convex QP can be classified as [28, 29]:

- Potential reduction algorithms
- Path following methods, such as the short step path following algorithm and the predictor-corrector algorithm
- Affine scaling algorithms
- Infeasible interior point algorithms

The various algorithms that use the primal-dual framework differ in the way that they choose the starting point, the centering parameter, the step length, and also in their computational complexity. In 1989 Mehrotra described a practical algorithm which is considered the most efficient algorithm for LP and convex QP; his work appeared in 1992 [30].

Mehrotra's predictor-corrector algorithm builds on the theory of all primal-dual interior point algorithms together with other ideas from optimization and numerical analysis. It also incorporates a number of heuristics that have been developed during ten years of computational experience. Another key ingredient is the infeasible initial point [29]. Mehrotra's algorithm can be extended to convex QP problems. This has made it attractive to many applications such as optimal

control and model predictive control [31, 32, 33]. Mehrotra's algorithm has been chosen to solve the optimal control problem inherent in the *DMC* controller of the bleaching process.

4.5 Mehrotra predictor corrector algorithm for convex QP

The optimal control problem involved in the *DMC* controller for the bleaching process is a convex QP problem with only inequality constraints. The primal problem can then be expressed as:

$$\min_{x} \quad f(x) = \tfrac{1}{2}x^T Qx + c^T x \tag{4.7a}$$

$$\text{subject to} \quad Ax \leq b \tag{4.7b}$$

where $Q \in R^{n\times n}$ is positive semi-definite matrix, $A \in R^{m\times n}$, $b \in R^m$, and $c \in R^n$.

The strong lagrangian dual (QD) problem can be expressed in terms of the lagrange multiplier λ as:

$$\max_{x} \quad d(x,\lambda) = -\tfrac{1}{2}x^T Qx - b^T\lambda \tag{4.8a}$$

$$\text{subject to} \quad Qx + c + A^T\lambda = 0 \tag{4.8b}$$

$$\lambda \geq 0 \tag{4.8c}$$

Given a slack variable for the inequality constraints, $s = Ax - b$, the Karush-Kuhn-Tucker (KKT) conditions for QP can be written as:

$$Qx + c + A^T\lambda = 0 \tag{4.9a}$$

$$Ax + s - b = 0 \tag{4.9b}$$

$$s_i\lambda_i = 0,\ i = 1, 2, \ldots, m \tag{4.9c}$$

$$(\lambda, s) \geq 0 \tag{4.9d}$$

The KKT conditions can be written in terms of the primal-dual feasible set $\mathcal{F}$ as follows:

$$\mathcal{F} = \{(x,\lambda,s) | F(x,\lambda,s) = 0, (\lambda,s) \geq 0\} \tag{4.10a}$$

$$\text{where } F(x,\lambda,s) = \begin{bmatrix} Qx + c + A^T\lambda \\ Ax + s - b \\ \Lambda Se \end{bmatrix} \tag{4.10b}$$

where

$$\Lambda = diag(\lambda_1, \lambda_2, \cdots, \lambda_m)$$
$$S = diag(s_1, s_2, \cdots, s_m),\ e = (1, 1, \cdots)$$

Based on the KKT conditions, $x^\star$ is an optimal feasible solution for QP if and only if the three optimality conditions hold [28, 29]:

- Primal feasibility: $x^\star$ is feasible for QP.
- Dual feasibility: $x^\star, \lambda^\star$ are feasible for QD.
- Complimentary slackness: $f(x^\star) = d(x^\star, \lambda^\star)$

Mehrotra's algorithm, like many interior point algorithms, generates a sequence of infeasible iterates along the central path, which connects the analytic center and the solution set. The central path for convex QP is defined by the following:

$$\mathcal{C} = \{(x, \lambda, s) \in \mathcal{F} |\ \Lambda S = \mu e, \mu \geq 0\} \tag{4.11}$$

where $\mu = \frac{\lambda^T s}{m}$ is the duality gap, which is a measure of the desirability of each point in the search space. The search direction at each iterate consists of three components [29]:

- an affine-scaling "predictor" direction which is the pure newton direction for the function $F(x, \lambda, s)$ defined in equation 4.10b,
- a centering term whose size is governed by the adaptively chosen centering parameter σ; if the affine-scaling direction makes good progress in reducing the duality measure μ while remaining inside the positive orthant $(\lambda, s) > 0$, a little centering is needed and a small value is assigned to σ, on the other hand, a significant amount of centering is needed and σ is chosen near 1, if the affine-scaling direction is only a short distance from violating the constraint $(\lambda, s) > 0$, and
- a corrector direction that attempts to compensate for the nonlinearity in the affine-scaling direction.

Having briefly discribed Mehrotra's predictor-corrector algorithm for convex QP, the general steps of the algorithm can be specified as follows [30, 26]:

1. Choose a starting point (x_0, λ_0, s_0) such that $(\lambda_0, s_0) > 0$.

   The approach that was proposed by Mehrotra for estimating an initial infeasible point for linear programming LP [30], is extended for the convex QP problem as follows:

$$\tilde{x} = (A^T A)^{-1} A^T b \tag{4.12a}$$

$$\tilde{\lambda} = A(A^T A)^{-1} b \tag{4.12b}$$

$$\tilde{s} = b - A\tilde{x} \tag{4.12c}$$

$$\delta\lambda = max(-1.5min(\tilde{\lambda}), \epsilon) \tag{4.12d}$$

$$\delta s = max(-1.5min(\tilde{s}), \epsilon) \tag{4.12e}$$

$$\tilde{\delta\lambda} = \delta\lambda + 0.5\frac{(\tilde{\lambda} + \delta\lambda)^T(\tilde{s} + \delta s)}{\sum_{i \leq m}(\tilde{s}_i + \delta s_i)} \tag{4.12f}$$

$$\tilde{\delta s} = \delta s + 0.5\frac{(\tilde{\lambda} + \delta\lambda)^T(\tilde{s} + \delta s)}{\sum_{i \leq m}(\tilde{\lambda}_i + \delta\lambda_i)} \tag{4.12g}$$

$$x_0 = \tilde{x} \tag{4.12h}$$

$$\lambda_0 = \tilde{\lambda} + \tilde{\delta\lambda} \tag{4.12i}$$

$$s_0 = \tilde{s} + \tilde{\delta s} \tag{4.12j}$$

   where ϵ is a small positive constant. Mehrotra et al discussed the validity and the properities of his approach [30]. Lustig, Marsten, and Shanno suggested a different approach for generating the initial point and stated that the predictor-corrector algorithm is quite sensitive to the initial guess to the optimal solution [34].

2. Evaluate the stopping criteria: Given the feasibility residuals $r_b = Ax + s - b$ and $r_c = Qx + c + A^T\lambda$, the following three condition must hold:

   - Primal feasibility: $\|r_b\|/(1 + \|b\|) \leq \epsilon$
   - Dual feasibility: $\|r_c\|/(1 + \|c\|) \leq \epsilon$
   - Complementary slackness: $|x^T Qx + b^T\lambda + c^T x| \leq \epsilon$

3. Compute the affine-scaling direction: It can be obtained from the first order approximation of the function $F(x, \lambda, s)$ defined in equation 4.10b.

$$\begin{bmatrix} Q & A^T & 0 \\ A & 0 & I \\ 0 & S & \Lambda \end{bmatrix} \begin{bmatrix} \Delta x_{aff} \\ \Delta \lambda_{aff} \\ \Delta s_{aff} \end{bmatrix} = \begin{bmatrix} -r_c \\ -r_b \\ -\Lambda S e \end{bmatrix} \tag{4.13}$$

4. Compute steps to the boundary along the affine scaling direction:

$$\alpha_{aff} = max\{\alpha \in [0,1] | (\lambda, s) + \alpha(\Delta\lambda_{aff}, \Delta s_{aff}) \geq 0\} \tag{4.14}$$

In order to measure the efficiency of the affine-scaling direction, the duality gap attained from a full step to the boundary is defined as:

$$\mu_{aff} = \frac{(\lambda + \alpha_{aff}\Delta\lambda_{aff})^T(s + \alpha_{aff})s_{aff}}{m}$$

5. Compute the centering-corrector direction: The centering parameter σ is computed from the following heuristic:

$$\sigma = (\frac{\mu_{aff}}{\mu})^3$$

Given a centering parameter $\sigma \in [0, 1]$, the centering-corrector direction is estimated by solving the following linear system:

$$\begin{bmatrix} Q & A^T & 0 \\ A & 0 & I \\ 0 & S & \Lambda \end{bmatrix} \begin{bmatrix} \Delta x_{cc} \\ \Delta \lambda_{cc} \\ \Delta s_{cc} \end{bmatrix} = \begin{bmatrix} 0 \\ 0 \\ \mu\sigma e - \Delta\Lambda_{aff}\Delta S_{aff} \end{bmatrix} \tag{4.15}$$

where $\Delta\Lambda_{aff} = diag(\Delta\lambda_{aff})$, and $\Delta S_{aff} = diag(\Delta s_{aff})$ are diagonal matrices.

6. Compute the search direction:

$$\Delta x = \Delta x_{Aff} + \Delta x_{cc} \tag{4.16a}$$

$$\Delta \lambda = \Delta \lambda_{Aff} + \Delta \lambda_{cc} \tag{4.16b}$$

$$\Delta s = \Delta s_{Aff} + \Delta s_{cc} \tag{4.16c}$$

7. Determine the step size and update:

$$\alpha_{max} = argmax\{\alpha \in [0,1] | (\lambda, s) + \alpha(\Delta\lambda, \Delta s) \geq 0\} \tag{4.17}$$

$$x = x + min(1, 0.995\alpha_{max})\Delta x \tag{4.18a}$$

$$\lambda = \lambda + min(1, 0.995\alpha_{max})\Delta\lambda \tag{4.18b}$$

$$s = s + min(1, 0.995\alpha_{max})\Delta s \tag{4.18c}$$

8. Compute the duality gap $\mu = \frac{\lambda^T s}{m}$ and go to step 2.

When compared with other optimization methods and other interior point methods, the Mehrotra's predictor corrector algorithm is to date the most computationally efficient method for solving large scale convex QP and other convex programming classes as computational and numerical analysis studies have shown [30, 34].

4.6 Hot starting

Model predictive control solves a sequence of similar optimal control problems in succession. These problems vary only slightly from one problem to the next. It is highly desirable that the optimization algorithm should be able to take advantage of this fact. The information would be used to choose good starting values for all the variables. The process of using the information is called hot starting.

Several studies proposed different approaches for applying hot starting to interior point methods [29, 32, 35]. One approach is to use a shifted version of one of the earlier interior point iterates from the previous problem. Since the interior point algorithm tends to follow the central path, this strategy produces an iterate which is close to the central path for the new optimal control problem.

In the presence of disturbances, the previous solution may have little relevance to the new optimal control. A starting point in this case can be constructed from the unconstrained solution or from a cold start using a well centered point. It has been shown that for LP problems, interior point methods gain about a factor of three in compute time efficiency when they are hot started in comparison with cold start (no prior information).

4.7 Interior point methods vs. active set methods

The interior point approach has a number of advantages over the active set approach from a computational point of view [27, 26]. It is difficult for the active set algorithm to exploit any structure inherent in the QP problem without redesigning most of its complex linear algebra operations. In an interior point algorithm, on the other hand, the only complex linear algebra operation is the solution of the linear system. Hence the interior point approach can exploit fully the properties of the system arising for each problem class.

The active set approach is very efficient for small and medium scale problems, whereas the interior point approach is efficient for large scale problems. The active set approach requires much less execution time than the interior point approach in many contexts, especially when a hot starting technique is applied and the problem is generic enough that not much benefit is gained by exploiting its structure. However, an active set approach requires large number of steps in which each search direction is relatively inexpensive to compute, while interior point approach takes a smaller number of more expensive steps.

Chapter 5

Simulation and Implementation Results

5.1 The bleaching process controller design issues

The mechanical pulp bleaching process at Irving Paper mill is a very complex process. For the sake of simplicity, the bleaching process is handled as a $SISO$ system whose input and output are the peroxide dosage and the finel pulp brightness respectively. Since the bleaching process has a variable delay time, a delay time esimator is embedded in the controller. The DMC strategy is used to control the bleaching process with a control horizon $N_U = 1$ and a prediction horizon N_P, which is a function of the estimated delay time T_d to compensate for the time-variability of the process:

$$N_P(k) = T_d(k) + N_{Po}$$

where $N_{Po} = 4\tau$ is the prediction horizon of the bleaching process whose time constant is τ. Identification studies have shown that the gain of the process is nonlinear and depends on the peroxide dosage. A gain scheduling technique has been applied in the controller to cope with nonlinear gain of the process. Figure 5.1 illustrates the relationship between the brightness gain and the peroxide dosage. A combination of a Smith predictor and feed-forward techniques has been embedded in the controller to compensate for the incoming pulp brightness variations, and hence improve the performance of the controller. Figure 5.2 shows the scheme of the DMC controller.

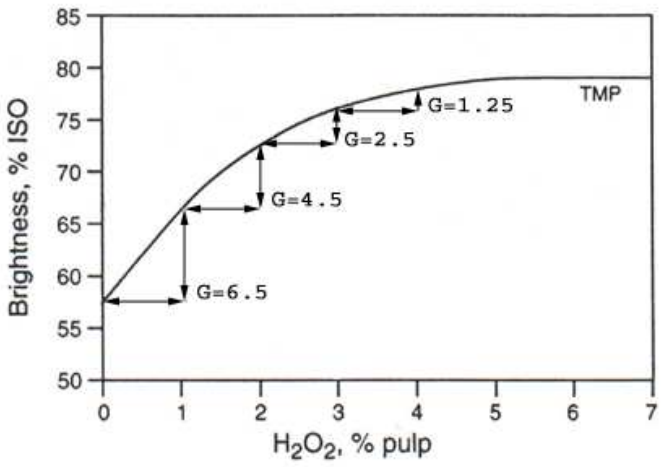

Figure 5.1: The nonlinear brightness gain with respect to peroxide dosage.

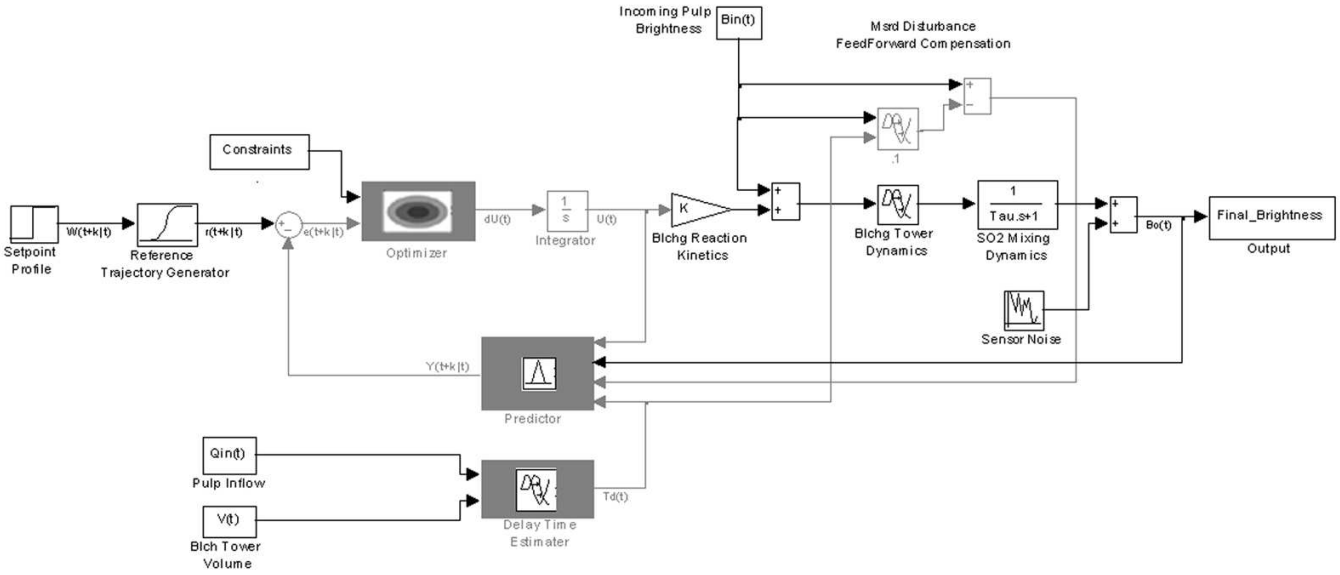

Figure 5.2: The bleaching process DMC controller.

5.2 Nominal performance

The objective of this simulation is to study the behaviour of the closed loop system in terms of its nominal performance. The *DMC* controller parameters were chosen appropriately, the prediction horizon $N_P = 4\tau + T_d(k)$ where τ is the time constant of the bleaching process, the control horizon $N_U = 1$, the peroxide dosage constraints $0.0\% \leq U \leq 0.5\%$, and the slew rate constraints $|du| \leq 0.1\%/minute$. It is important to mention that all the process parameters (i.e., the pulp brightness and the peroxide dosage) in this simulation are incremental ones without any bias.

When a stair signal is applied to the reference input at different points on the variable delay time function (top trace), the final brightness exactly tracks the reference brightness signal at different delay times (bottom trace) as illustrated in figure 5.3. This implies that the *DMC* controller works well even though the delay time is varying.

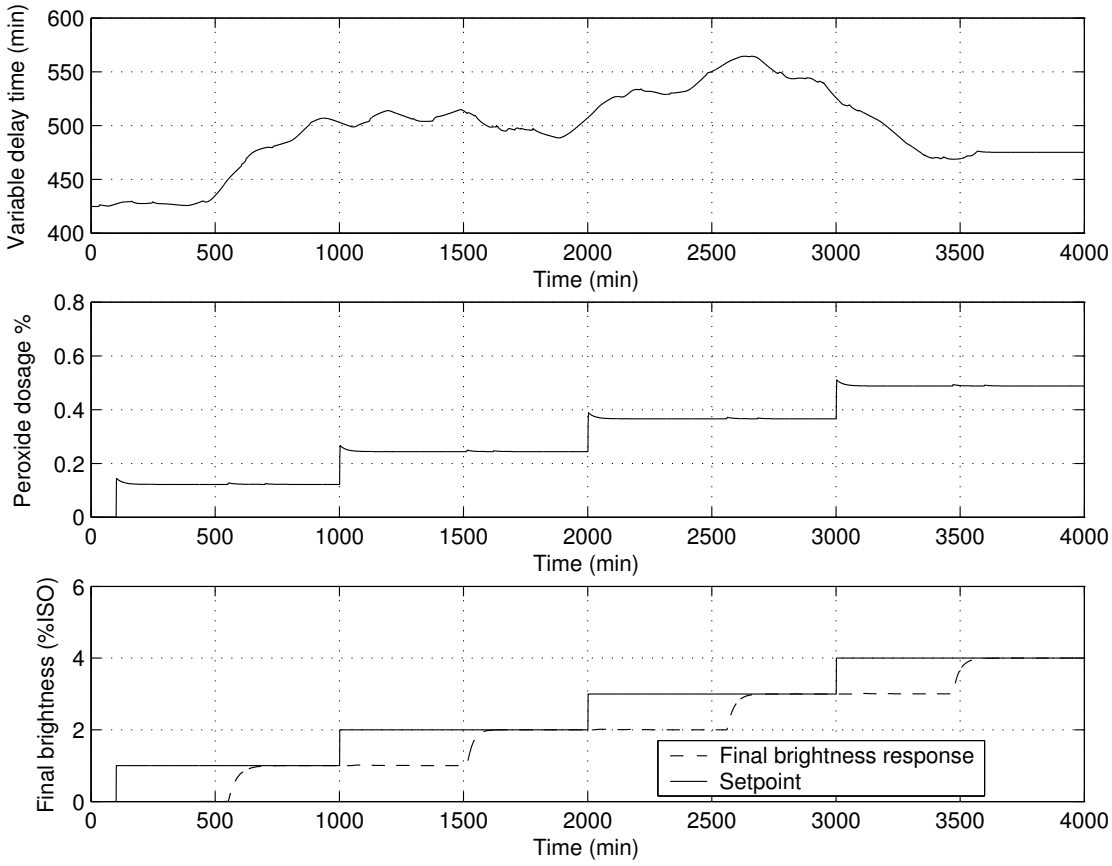

Figure 5.3: System response to stairs signal at different delay times

In order to study the behaviour of the system in the presence of disturbances, a disturbance in the incoming pulp brightness was applied at the time instant $t = 2000\ min$ as shown in figure 5.4. When there is no feedforward compensation included in the *DMC* controller, the effect of the disturbance appears on the final brightness response (dash-dotted line) after some delay time and lasts for a long time (more than 500 min) before it is completely rejected. However the disturbance is immediately rejected when the feedforward plus smith predictor technique is included in the *DMC* controller (solid line), and the system performance is improved in comparison with the previous case. This is obvious from the peroxide dosage response (control signal) where it responds to the disturbance earlier in the feedforward compensated case.

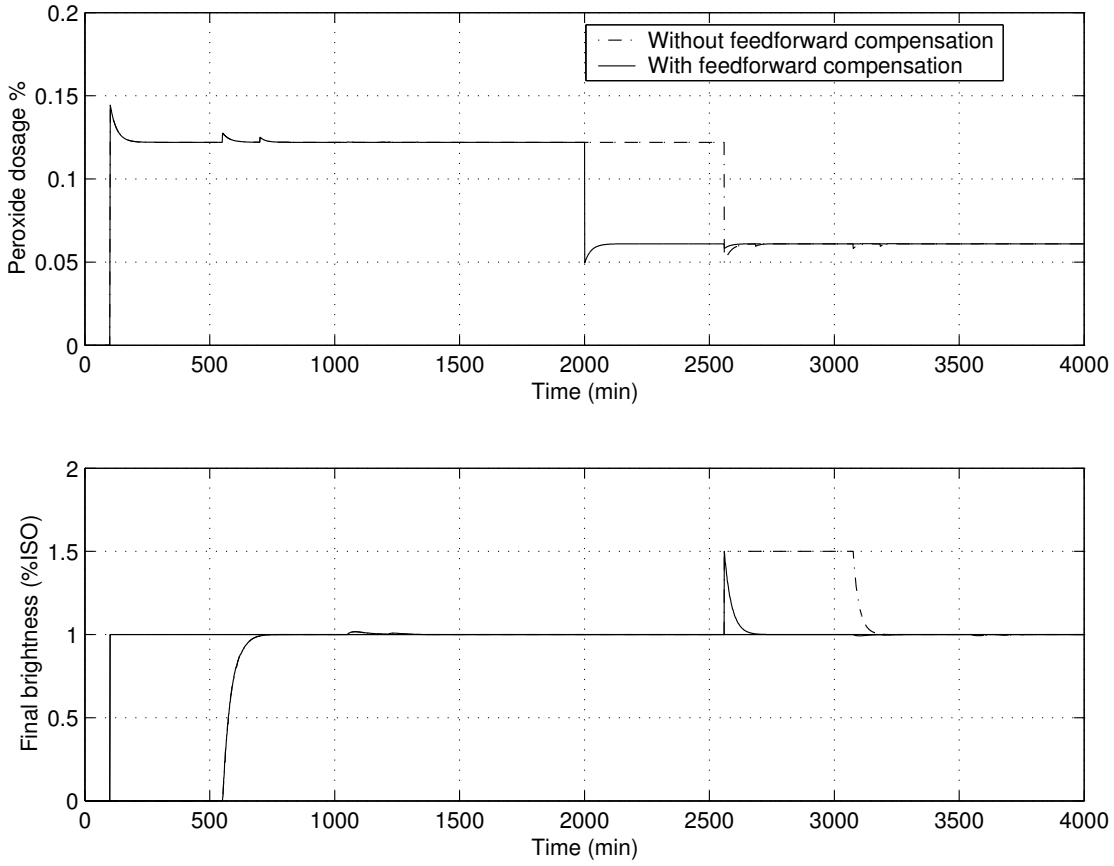

Figure 5.4: The effect of disturbance rejection on the system performance

5.3 Robust performance

This simulation is aimed at studying the behaviour of the system in the presence of parameter uncertainties in the bleaching process model. The parameters of the *DMC* controller are still the same as the previous simulation. It is important to mention that all the process parameters (i.e., the pulp brightness and the peroxide dosage) in this simulation are incremental ones without any bias.

As illustrated in figure 5.5, when the process has a gain uncertainty of $\mp 20\%$ (dash-dotted line for the $+20\%$ case and dotted line for the -20% case), the final brightness response to a step at the reference input is markedly different from the nominal case. The final brightness does not track the reference for a fairly long time (an additional process delay time). It finally corrects itself, steping up or down according to the sign of the uncertainty, and eventually gets back to track the reference. This implies that the *DMC* controller sets the peroxide dosage (top trace) for the nominal case for some time, and then it corrects the dosage according to the sign and size of the gain uncertainty.

The system response does not show much difference, when the time constant of the bleaching process is perturbed by $\mp 20\%$, as can be seen in figure 5.6 (dash-dotted line for the $+20\%$ case and dotted line for the -20% case). The effect of uncertainty in the time constant on the final brightness (closed loop response) will change according to the sign and size of the time constant uncertainty, as shown.

As previous simulations have demonstrated, introducing uncertainty in the parameters of the delay-free part of the bleaching process has only led to moderate changes in the system performance, without affecting its stability. However, if there is an uncertainty in the delay time of the process, then both the performance and the stability of the closed loop system will be affected. When introducing a delay time uncertainty of $\mp 5\%$ in the process, as can be observed in figure 5.7 (dash-dotted line for the $+5\%$ case and dotted line for the -5% case), the final brightness starts to exhibit peaking, which only slowly decreases. In fact, the brightness response shows some "blips" every 500 minutes which will develop to a stable or unstable oscillation depending on the sign and size of the uncertainty as time elapses. In order to explain those blips let's consider the -5% case, in which the brightness response occurres earlier than it is supposed to. This implies that

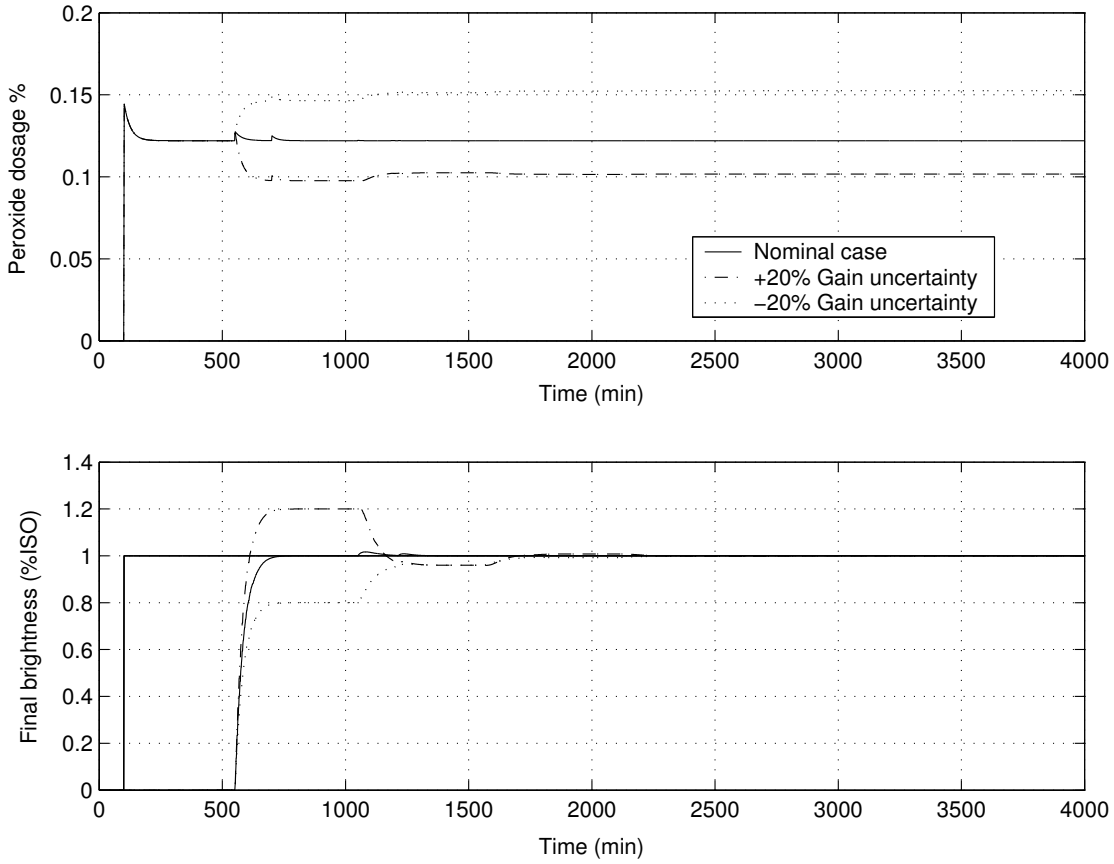

Figure 5.5: The system response to $\mp 20\%$ gain uncertainty.

the early measurement of the brightness will cause an error in the estimation of the free response in the *DMC* control algorithm. Consequently the future error between the predicted free response and the set point profile will no longer be zero, which causes a downward blip in the control action as time elapses. This will cause a blip in the brightness response after some delay time that will result in another error, and the story will be repeated every delay time, resulting in peaking. Fortunately the blips decay after some time, which indicates that the system is still stable. If the size of the delay time uncertainty is increased to $\mp 10\%$, the amplitude of the oscillation in both the final brightness response and the peroxide dosage is increased. The system in this situation becomes unstable for both uncertainty cases as illustrated in figure 5.8. It can be concluded that the delay time uncertainty must be small in order to obtain a high performance from the *DMC* controller and preserve its stability.

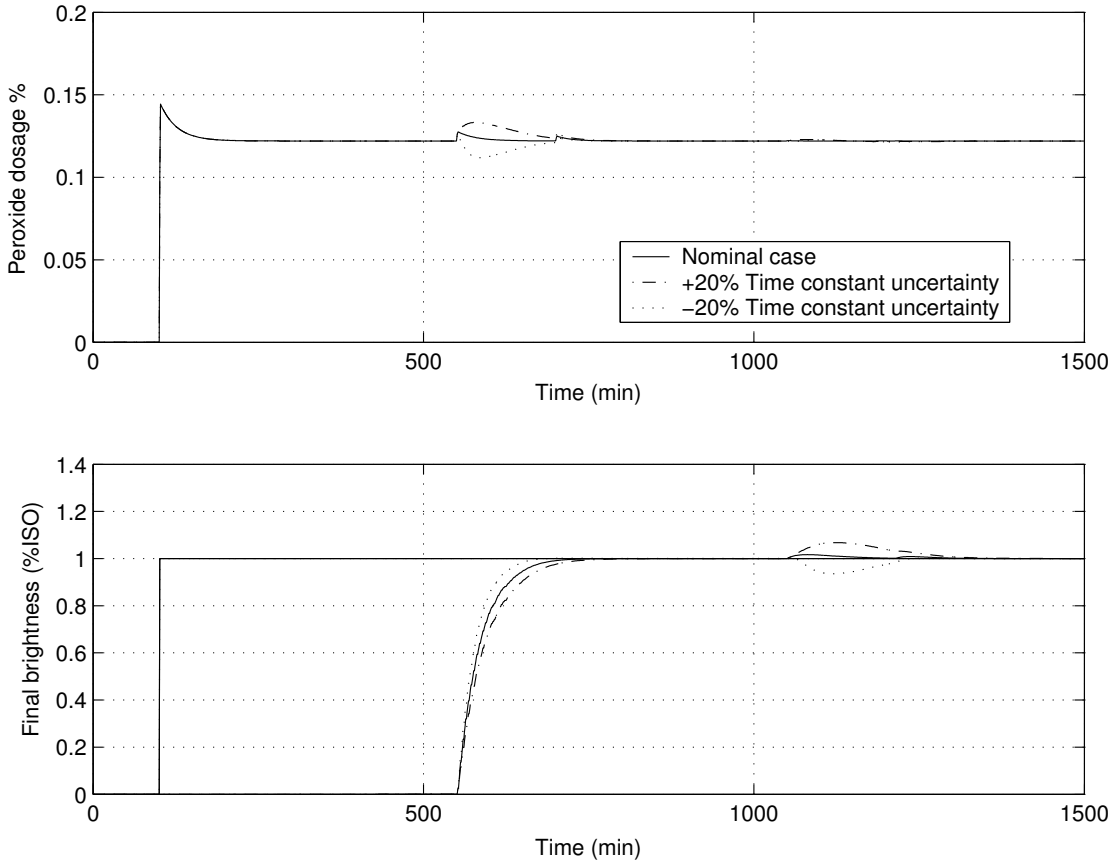

Figure 5.6: The system response to $\mp 20\%$ time-constant uncertainty.

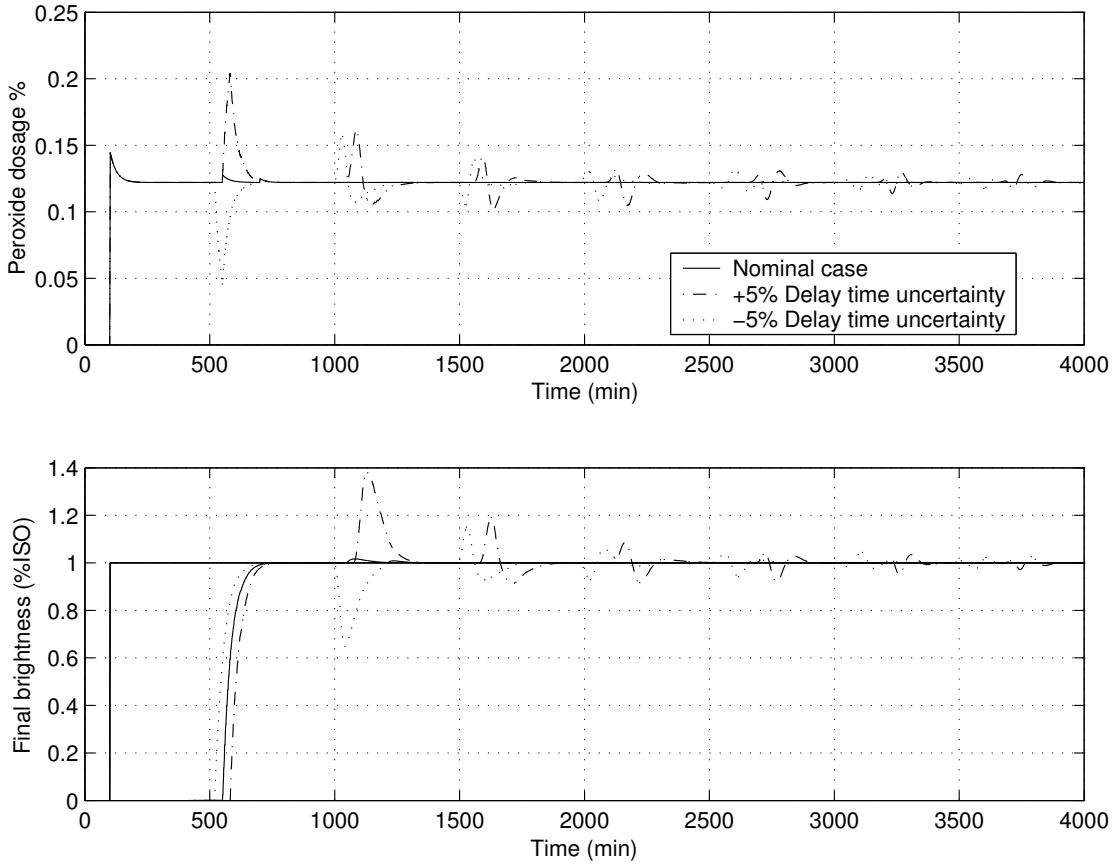

Figure 5.7: The system response to $\mp 5\%$ delay time uncertainty.

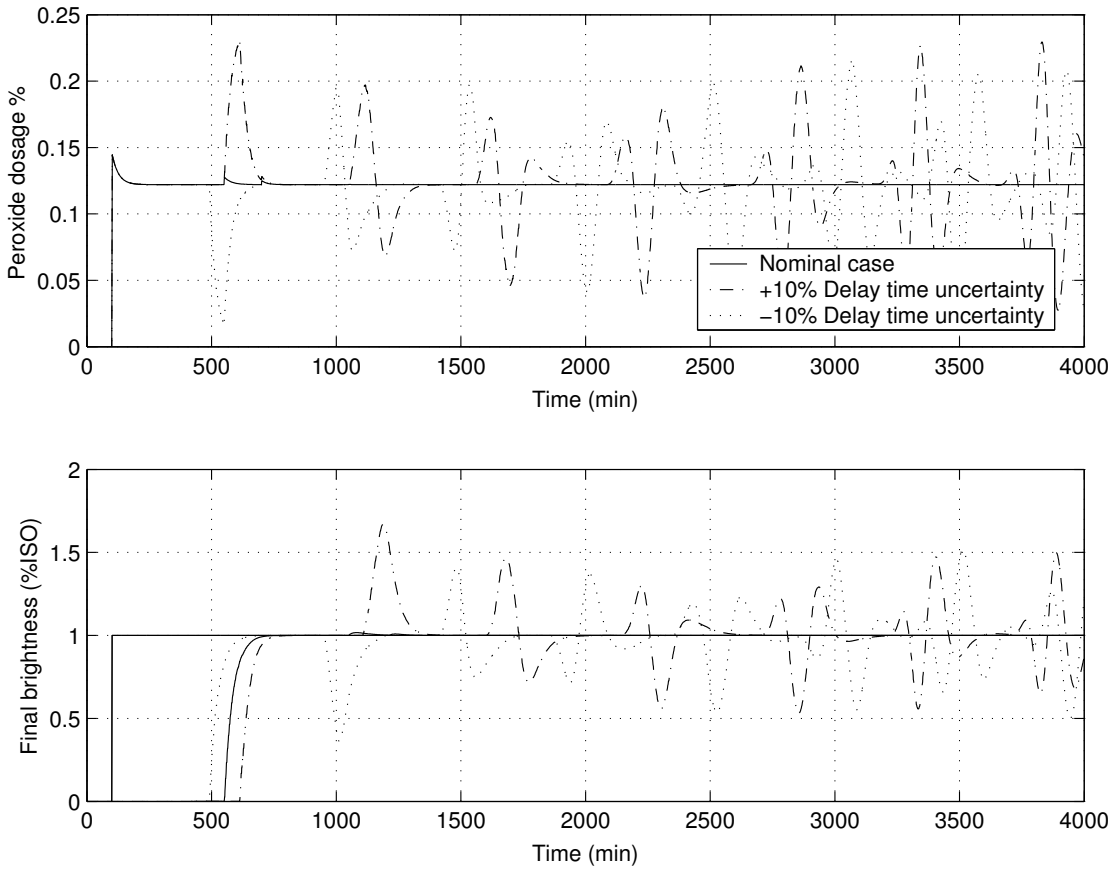

Figure 5.8: The system response to $\mp 10\%$ delay time uncertainty.

5.4 Implementation results

Simulation results have shown some very promising results in terms of the nominal performance of the closed loop system. However, those results were conservative when the system was simulated against different types of uncertainties (i.e., robust performance). The true performance of the *DMC* controller would only be revealed if it is implemented and tested on the real bleaching process at the Irving Paper mill. Therefore a control prototype was designed and implemented in the Irving Paper mill (refer to appendix B for more details about this implementation).

The technology was implemented as an advisor, so the tests were made in a semiautomatic way. This implies that the control program was not allowed to write the optimal peroxide dosage directly to the process, which guarantees smoothness of controlling the process without being affected by any undesirable actions from the controller.

5.4.1 *DMC* controller test: objectives and difficulties

Two tests have been done to validate the performance of the *DMC* controller in real time (i.e., during the normal operating the conditions of the bleaching process at Irving Paper mill). A set of objectives was defined to be met during the tests:

1. validation of the delay time estimator,
2. study of the effect of the incoming pulp brightness,
3. study of robustness w.r.t. T_d,
4. study of nonlinearity of the process, and
5. study of SO_2 effect.

The tests were done by applying a step change in the pulp brightness reference input and changing the hydrogen peroxide dosage according to the recommended dosage for the control advisor. However, working with real complex processes such as the bleaching process implies that difficulties and problems may take place and may degrade the performance of the controller during the tests.

One of the difficulties that contributed to the degradation of the controller performance is the high sensitivity of the bleaching process to the SO_2 dosage.

In fact the SO_2 dosage has a great influence on the pulp pH and the brightness measurement (refer to the second chapter for more details). Fortunately the SO_2 dosage was constant during the first test, which resulted in very promising results. However, the SO_2 dosage was varying during the second test, to compensate for the variation of the pulp pH, which severely degraded the performance of the DMC controller to the extent that there was no change in the final brightness when a step change was applied at the reference input.

Although the incoming pulp brightness sensor was repaired by the technical staff of Valmet Automation before making the tests, the sensor was not measuring the incoming pulp brightness properly. This implies that the study of the effect of the incoming pulp brightness (second objective) had to be cancelled during the tests.

Another less serious problem was the inaccurate measurement provided by the final pulp brightness sensor. In other words, there was a difference between the real brightness and the measured one, which resulted in a parametric uncertainty in the gain of the bleaching process model. Although the tests were done in a highly uncertain environment, the results of the first test revealed some very significant facts.

5.4.2 First test results

The test was done by applying a step change at the brightness reference input and changing the peroxide dosage of the real bleaching process according to the recommended dosage of the control advisor. The operators of the bleaching process at Irving Paper mill were asked to follow the recommended dosage by the control advisor as much as possible, in order to simulate nearly the closed loop behaviour of the DMC controller.

Figure 5.9 shows the dosages of the secondary bleaching process chemicals during the first test, where the silicate dosage was constant around 3% (middle plot). Fortunately the SO_2 (bottom plot) was remarkably constant, thus not degrading the performance of the DMC controller. The caustic dosage (top plot) was changed as the peroxide dosage changed (see figure 5.10), in order to meet a specified TA/H_2O_2 ratio.

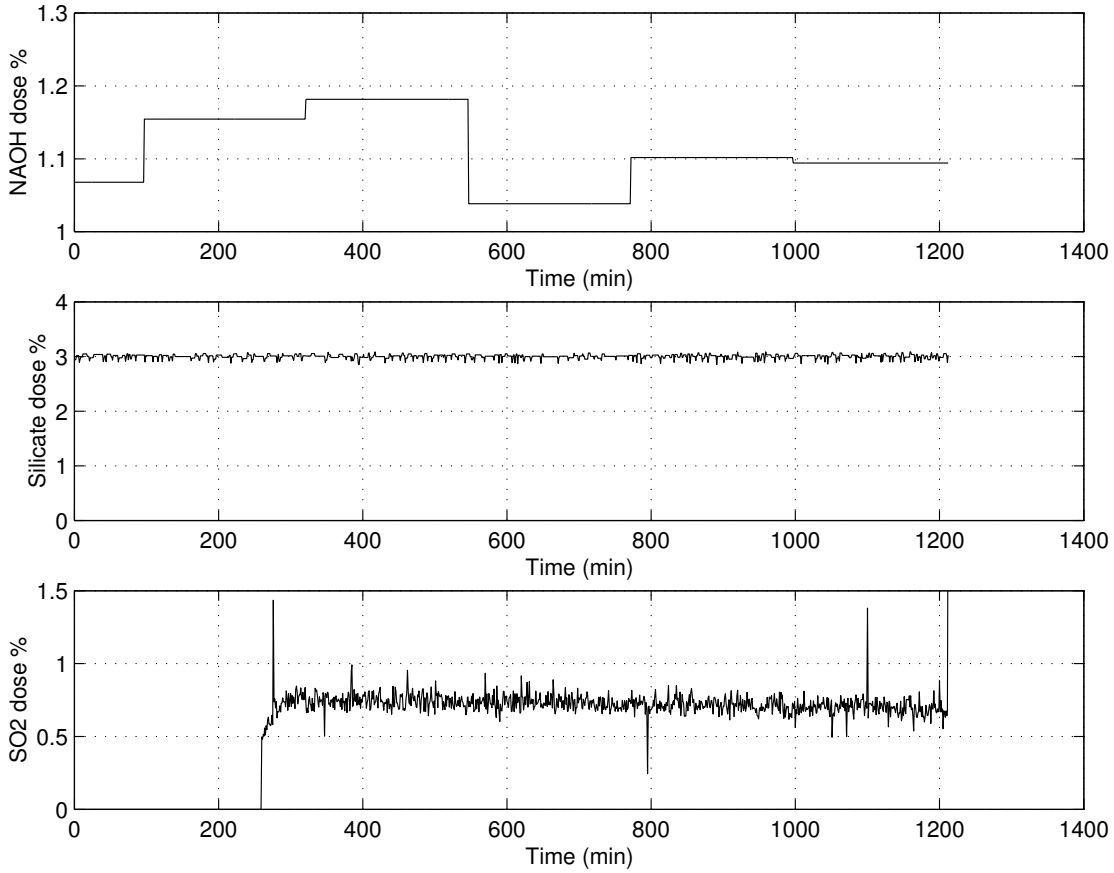

Figure 5.9: The dosages of secondary bleaching chemicals, first test.

Returning to the brightness controller, a step change of $4\%ISO$ was applied at the reference input at time instant $t = 418$ minutes and the setpoint was adjusted to corresponde to $65.827\%ISO$ (i.e., the initial conditions), as demonstrated in figure 5.10. The change in final brightness response (bottom plot) occurred at time instant $t = 700$ minutes. The figure also shows the recommended peroxide dosage by the control advisor (noisy trace, top plot) and the actual peroxide dosage applied to the real bleaching process (solid trace, top plot).

5.4.3 Discussion and analysis of the first test results

Having shown the results of the first test, the analysis of these results would reveal whether the objectives of this test have been met or not. The initial conditions of the peroxide dosage and the final pulp brightness before making the test were 0.864% and $65.827\%ISO$ respectively. Both the recommended peroxide dosage

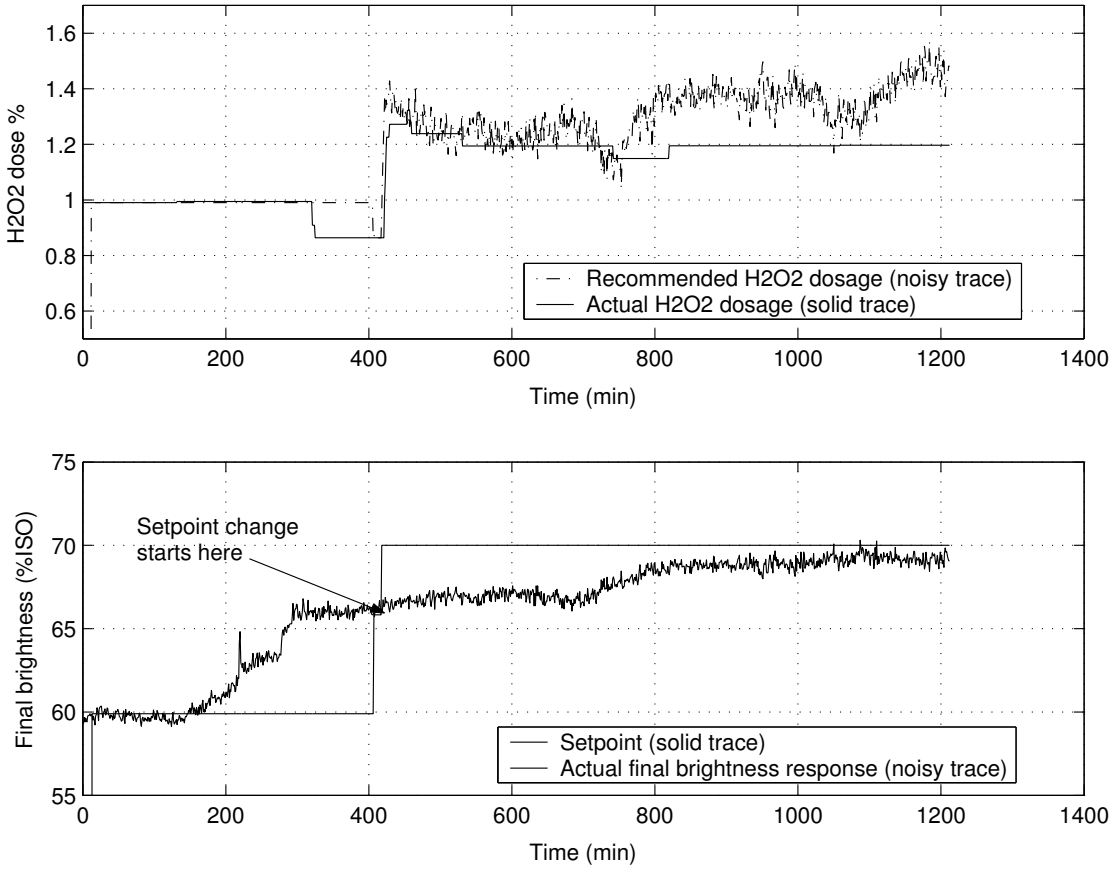

Figure 5.10: The final pulp brightness to a step change at the reference, first test.

(noisy trace, top plot) and the actual one (solid trace, top plot) were simulated by using a brightness model that has the same parameters used in the control advisor. The simulated brightness responses (solid and dashed traces, bottom plot) were then plotted along with the measured final brightness (noisy trace, bottom plot) after removing the bias as figure 5.11 demonstrates.

Clearly the bottom plot reveals two interesting and yet significant observations:

1. It is obvious that both the simulated and the measured brightness responses failed to track the set point. This due to the inaccurate measurement of the final brightness sensor, which resulted in an apparent gain uncertainty in the bleaching process. However, the *DMC* controller increased the peroxide dosage (noisy trace, top plot) at time instant $t = 770$ minutes to compensate for the gain uncertainty. As a result, the simulated brightness response (dashed trace, bottom plot) was changed at time instant $t = 1090$ minutes to attempt

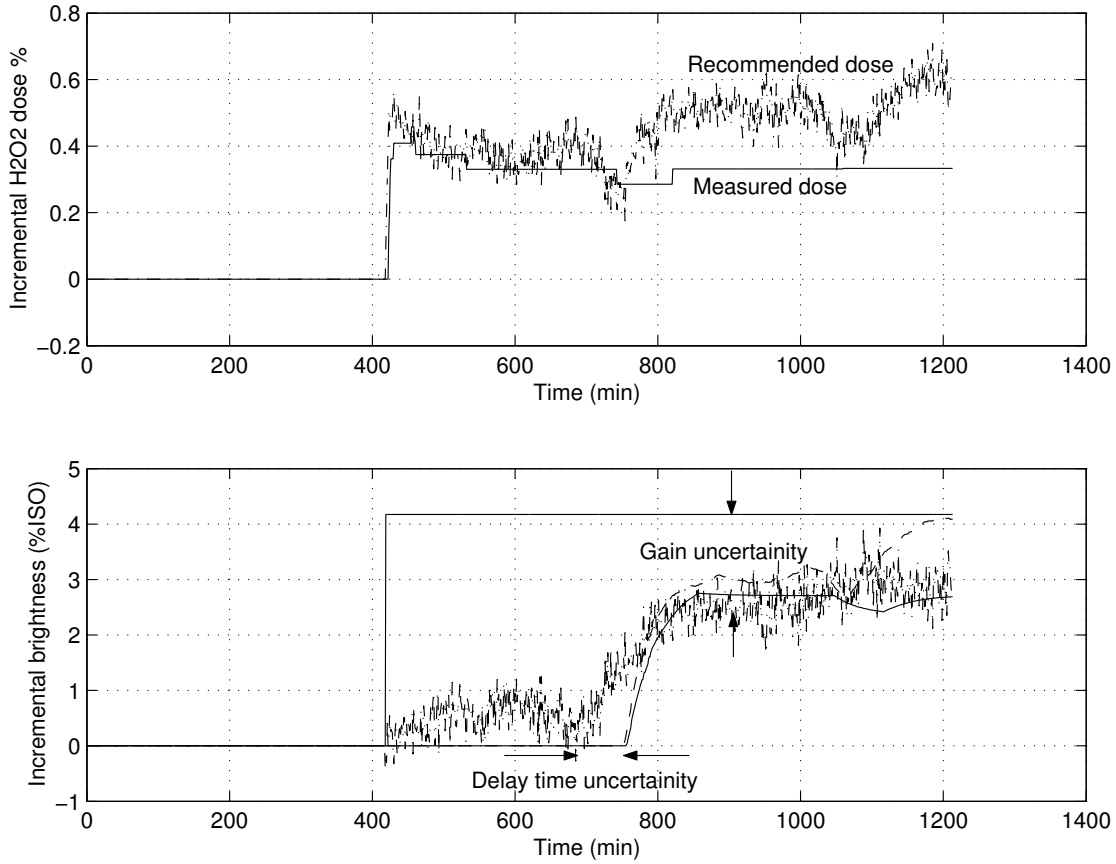

Figure 5.11: The final pulp brightness responses after removing the bias, first test.

to track the set point. This indicates that the *DMC* controller can handle gain uncertainty, as the robust performance simulation has exactly shown. But the real peroxide dosage (solid trace, top plot) was not allowed to follow the recommended peroxide dosage exactly for economic considerations.

2. It is interesting to observe that the change in the real brightness response (noisy trace, bottom plot) occurred earlier than it was supposed to. In other words, it should have occurred at the same time as the simulated brightness response (dashed trace, bottom plot). This implies that a delay time uncertainty has happened during the test. The effect of the uncertainty is also clear in the recommended peroxide dosage where a downward blip took place at the same time of the uncertainty. This result is identical to what was observed in the robust performance simulations.

As far as the delay time estimation is concerned, figure 5.12 demonstrates the

results, where the delay time estimator used the pulp inflow (top plot) and the pulp volume in the bleaching tower (middle plot) to estimate the delay time online in real time (bottom plot).

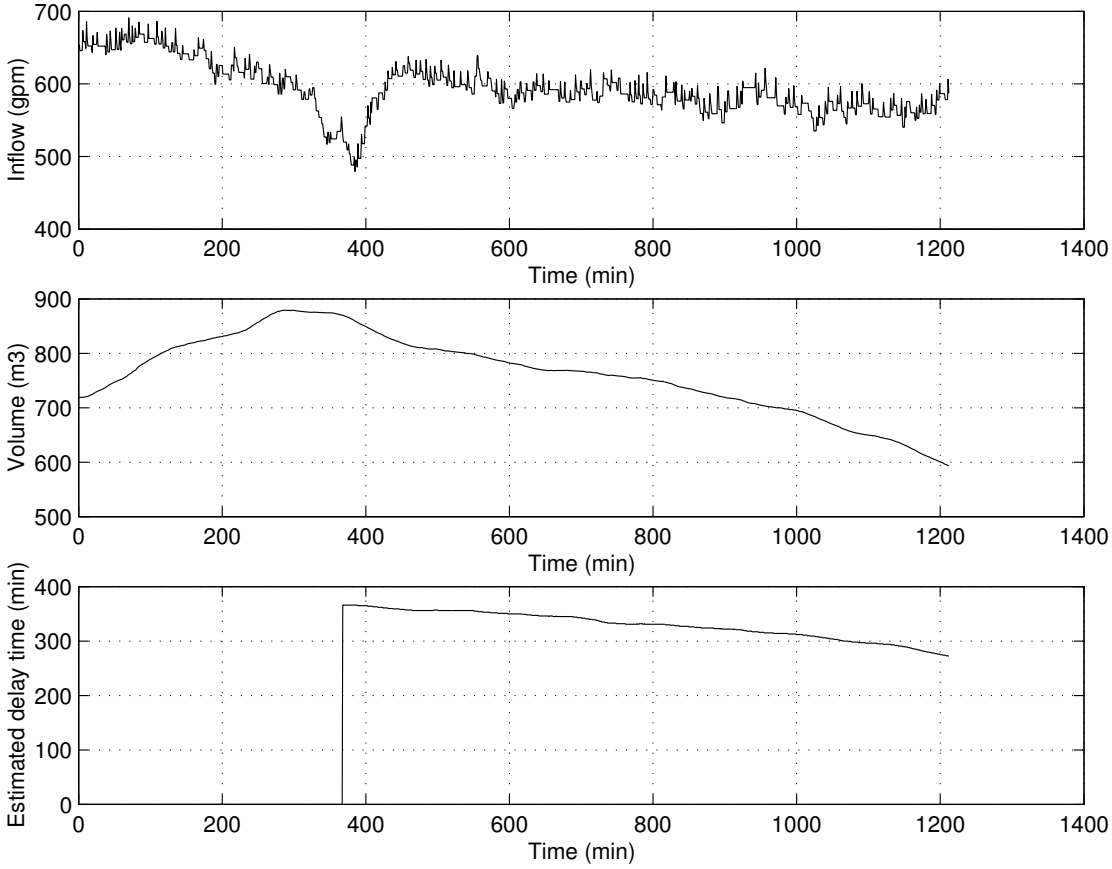

Figure 5.12: The estimated delay time, first test.

The reason for the delay time uncertainty is because the pulp level inside the bleaching tower was decreasing during the test, which caused the brightness change to happen earlier than anticipated. This, in turn, raises questions about the performance of the delay time estimator for use in real time control.

The delay time estimator integrates the pulp outflow backward in time to estimate the delay time of the pulp leaving the bleaching tower (see section 2.4.1). Of course the estimated delay time in the case of decreasing pulp level in the bleaching tower will be larger than the actual delay time. This suggests that the estimator should integrate the pulp outflow forward in time, given the present time t is at the inlet of the bleaching tower rather than the outlet. This can be mathematically

expressed by:

$$\int_{t}^{t+Td(t)} Q_{out}(\tau)d\tau = V(t) \tag{5.1}$$

Figure 5.13 demonstrates this approach, where the delay time has been re-estimated offline by using the forward integration estimator (dashed trace, top plot), and then used to simulate the closed loop behaviour of the bleaching process when a step change is applied at the reference input. The new simulated brightness response (dashed trace, bottom plot) shows an improvement in terms of less delay time uncertainty compared to the old simulated brightness response (solid trace, bottom plot). However, the forward delay time estimator is physically unrealizable in real time, due to the difficulty of predicting the pulp outflow over such long period of future time. It should be mentioned that further simulations and tests are required to confirm the last result.

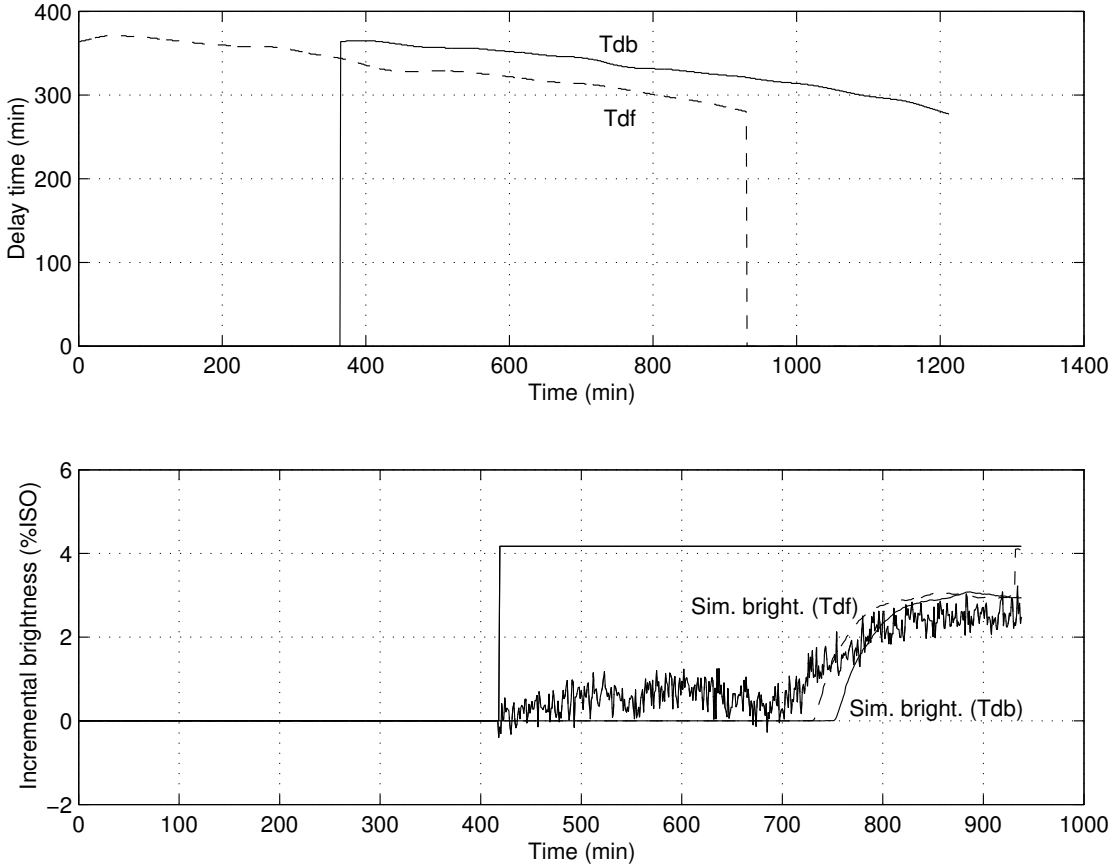

Figure 5.13: The effect of forward delay time estimation on the brightness response, first test.

Chapter 6

Thesis Observations

This research has revealed a lot of impressive observations and results about the mechanical pulp bleaching process at Irving Paper. A set of practical recommendations can be made of these observations, so that the performance of the bleaching process at the Irving Paper mill can be improved and the process efficiency can be raised. These observations and conclusions would also form a better framework for research and future studies to enhence the bleaching process at Irving Paper.

6.1 Summary and conclusions

1. The mechanical pulp bleaching process at Irving Paper mill has been thoroughly studied, analysed, and modelled.
2. Hydrogen peroxide dosage, caustic dosage, SO_2 dosage, incoming pulp brightness, and pulp consistency are considered the most important factors that have a great impact on the bleaching process.
3. Since the purpose of this research is to study the possibility of controlling the bleaching process, most chemical dosages were assumed to be constant during the bleaching reaction, and only the hydrogen peroxide dosage has been focussed on, for simplicity.
4. Simulation results and identification studies have shown that the bleaching process can be modelled a first order dynamics plus a variable delay time, where the peroxide dosage is the input and the final pulp brightness is the output. Pulp consistency and incoming pulp brightness can be considered as measurable disturbances.
5. A delay time estimator which is based on the backward integration of the pulp inflow was used in the identification studies to tackle the variable delay time challenge. Simulations demonstrated the estimator reliability when it is used offline for identification purposes.
6. Although the gain of the peroxide bleaching process is a nonlinear function of the peroxide dosage, identification studies have shown that the bleaching process at Irving Paper mill can be considered to be a linear process with a gain of 8.2 and a time constant of $50 - -60$ minutes, if the hydrogen peroxide dosage is less than 1.4%.

7. A model predictive control (*MPC*) strategy was chosen to control the process, due to its challenging characteristics when compared with processes for which traditional control methods (e.g., the *PID* control method) are effective. The bleaching process was considered to be linear when the *DMC* controller was designed.

8. A state of the art of optimization algorithm i.e., an interior point method, was incorporated in the controller for practical and industrial considerations (i.e., constraints on process variables).

9. Simulation studies on the nominal performance of the *DMC* controller have shown impressive results. However, results were acceptable in the case of robust performance simulations only if the delay time uncertainty was less than 8%.

10. An industrial control prototype was designed to implement the *DMC* controller in the real bleaching process, and to study its performance in real time.

11. Although the implementation and the testing phase had some practical problems (inaccurate brightness measurements and other problems), the test results were identical to the simulation results. This implies that the *DMC* controller performance was very acceptable during the tests. The analysis of the implementation results have shown that the delay time estimator was unreliable for real time control purposes.

12. A new delay time estimator which is based on the integration of the long horizon predicted pulp outflow, is proposed. Simulations have shown that the *DMC* controller performance can be improved when such an estimator is incorporated in the controller. However, the proposed estimator is physically unrealizable without good long-term prediction of pulp outflow.

13. Identification and implementation results have shown that SO_2 dosage has a great impact on the brightness measurement and pulp pH as well. This implies that the control of the pulp pH would improve both the efficiency of the bleaching process and the quality of the produced paper.

6.2 Future work

1. Since the final brightness measurement has shown a high sensitivity to the SO_2 dosage variations, a new model structure of the bleaching process that addresses the SO_2 dosage and the pulp pH, would form a better framework for research and future studies. The new proposed model must be a 2×2 multivariable model, where the hydrogen peroxide and the SO_2 dosages are the inputs. The final pulp brightness and pulp pH are the outputs of the new model. Pulp consistency and incoming pulp brightness can be considered measurable disturbances, which can be compensated by using a combination of feed forward control and smith predictor. Irving Paper has decided to upgrade the *TDC 3000 DCS* system and to improve the pulp pH control by installing a new pH sensor and a bigger SO_2 valve. This may enhance the future research and make it more successful. As far as the *DMC* controller is concerned, the controller itself does not require a lot of modification, since the *MPC* control strategy can be extended to handle multivariable cases easily.

2. The backward delay time estimator can be incorporated in the proposed multivariable *DMC* controller if and only if both pulp inflow and outflow are guaranteed to vary slowly or predictably. In other words, the rate of change of the pulp level in the bleaching tower should not be high or it should follow a planned schedule. The performance of the *DMC* controller in this case would be acceptable. However, if the rate of change of the pulp level in the bleaching tower is fast, then a state event handler can be incorporated in the controller. If the rate is acceptable then the handler would switch the *DMC* controller on, otherwise, the process is controlled manually. A final scenario would be to schedule the pulp outflow in the future, so that the prediction of the pulp outflow would be practically realizable and the forward delay time estimator can then be incorporated in the proposed controller.

3. The multivariable nature of the proposed *DMC* controller may place a large burden on the optimizer incorporated in the controller, because of the bigger size of the optimal control problem being solved in the controller. Future research may address the use of warm starting techniques and the use of sparse

cholesky algorithms to solve the augmented system of the linear equations. This would significantly increase the efficiency and the speed of the optimizer.

Bibliography

[1] J. R. Persley and R. T. Hill, "Peroxide bleaching of (chemi)mechanical pulps", *from Pulp bleaching principles and practice Ed. by Dence, Carlton W. and Reeve, Douglas W.*, pp. 457–489. Atlanta, Ga: TAPPI Press, 1996.

[2] Z. Li and G. Court, "Private communication and meeting with Irving Paper Ltd., St. John, N.B." July 2000, Jan 2001, Nov 2001, April 2002.

[3] C. W. Dence and D. W. Reeve, *Brightness: basic principles and measurement from pulp bleaching principles and practice*, pp. 697–716. Atlanta, Ga: TAPPI Press, 1996.

[4] Valmet Automation Kajaani Ltd., Kajaani, Finland, *Kajaani Cormec-C/M brightness sensor operating and maintenance manual*, November 1996.

[5] N. J. Sell, *Process control fundamentals for the pulp and paper industry.* Atlanta, GA: TAPPI Press, 1995.

[6] T. Soderstrom and P. Stoica, *System Identification.* New York: Prentice Hall, 1989.

[7] S. Moldenius and B. Sjogren, "Kinetic models for hydrogen peroxide bleaching of mechanical pulps," *Journal of wood chemistry and technology*, vol. 2, no. 4, pp. 447–471, 1982.

[8] C. Y. Wen and L. T. Fan, *Models for flow systems and chemical reactors.* New York: Marcel Dekker, Inc., 1975.

[9] X. Qian and P. Tessier, "Dynamic modelling and control of a hydrogen peroxide bleaching process," *Pulp and Paper Canada*, vol. 89, no. 9, pp. 81–85, 1997.

[10] L. Ljung, *System Identification, Theory for the user*. Upper Saddle River, NJ: Prentice Hall, 2nd ed., 1999.

[11] T. Andersson and P. Pucar, "Estimation of residence time in continuous flow system with dynamics," *Journal of process control*, vol. 5, no. 1, pp. 9–17, 1995.

[12] Y. Ni, "Private communication and meeting with Pulp and Paper Research Center, Fredericton, N.B." July 2000, Nov 2001.

[13] R. Ylinen and K. Zenger, "Computer aided anaylsis and design of time varying systems," in *Proc. of international workshop on computer aided systems theory, EUROCAST* (R. Pichler and R. Moreno Doas, eds.), (Kerms, Austria), pp. 73–95, Springer Verlag, 1991.

[14] K. Zenger, "Time-variable models for mixing processes under unsteady flow and volume," in *Proc. of 4th IFAC Sypmosium on dynamics of chemical reactors, distillation columns, and batch reactor* (J. B. Rawlings, ed.), (Oxford, UK), pp. 57–63, Pergamon Press, 1995.

[15] R. Ylinen and K. Zenger, "Simulation of variable delaysin material transport models," *Mathematics and computers in simulation*, vol. 37, pp. 57–72, 1994.

[16] C. R. Cutler and B. L. Ramarker, "Dynamic matrix control – a computer control algorithm," *Proceedings of the joint automatic control conference*, 1980.

[17] D. W. Clarke, C. Mohtadi, and P. S. Tuffs, "Generalized predictive control–part 1, the basic algorithm," *Automatica*, vol. 23, no. 2, pp. 137–148, 1987.

[18] M. Morari and J. H. Lee, "Model predictive control: past, present, and future," *Computers and chemical engineering*, vol. 23, no. 4–5, pp. 667–682, 1999.

[19] S. J. Qin and T. A. Badgwell, "An overview of industrial predictive control technology," in *Proc. of the 5th international conference on chemical process control (CPC-V)* (J. C. Kantor, C. E. Garcia, and B. Carnahan, eds.), vol. 93 of *AIChe Symposium series No. 316*, (Tahoe City, CA), pp. 232–256, 1996.

[20] C. Camacho, Eduardo F. Bordons, *Model predictive control*. Berlin, New York: Springer, 1999.

[21] J. E. Marshall, H. Gorecki, and A. Kroytowski, *Time delay systems, stability and performance criteria with applications*, pp. 201–227. New York: Ellis Horwood, 1992.

[22] J. E. Marshall, *Control of time delay systems*. London and New York: Peter Peregrinus Ltd., 1979.

[23] M. Morari and E. Zafiriou, *Robust process control*. Prentice Hall, new jersey ed., 1989.

[24] M. S. Bazaraa, H. D. Sherali, and C. M. Shetty, *Nonlinear programming: theory and algorithms*. New York: Wiley, 2nd ed., 1993.

[25] D. Luenberger, *Linear and nonlinear programming*. Reading, Mass: Addison-Wesley, 2nd ed., 1984.

[26] S. J. Wrght and J. Nocedal, *Numerical optimization*. New York: Springer, September 1999.

[27] F. A. Potra and S. J. Wright, "Interior point methods," *Journal of Computational and Applied Mathematics*, vol. 124, no. 1–2, pp. 281–302, 2000.

[28] Y. Ye, *Interior point algorithms: theory and analysis*. New York: Wiley, 1997.

[29] S. J. Wright, *Primal dual interior point methods*. Philadelphia: SIAM, 1997.

[30] S. Mehrotra, "On the implementation of primal dual interior point method," *Siam journal on optimization*, vol. 2, no. 4, pp. 575–601, 1992.

[31] S. J. Wright, "Applying new optimization algorithms to model predictive contol," in *Proc. of Chemical process control-V*, vol. 93 of *AIChE Symposium series no.316*, pp. 147–155, CACHE Publications, 1997.

[32] C. Rao, S. J. Wright, and J. Rawlings, "Applications of interior point methods to model predictive control," Preprint ANL/MCS-P664-0597, Mathematics and computer science division, Argonne National Laboratory, May 1997.

[33] A. Hansson, "A primal dual interior point method for robust optimal control of linear discrete time systems," *IEEE transactions on automatic control*, vol. 45, no. 09, pp. 1639–1655, 2000.

[34] I. J. Lustig, R. E. Marsten, and D. F. Shanno, "On implementing Mehrotra's predictor corrector method for linear programming," *SIAM Journal on Optimization*, vol. 2, no. 3, pp. 435–449, 1992.

[35] E. A. Yildirim and S. J. Wright, "Warm start strategies in interior point methods for linear programming," Preprint ANL/MCS-P799-0300, Mathematics and computer science division, Argonne national laboratory, March 2000.

Appendix A

Brightness Principles and Measurement

A.1 Meaning and interpretation of brightness

Brightness is a precisely defined measurement of reflectance of visible blue light of a pad of pulp sheets or an opaque stack of paper or paperboard. It indicates the level of success in a bleaching operation. Unbleached paper or board appears brown because blue light is absorbed by the chromophores. Bleaching chemically reduces the concentration of light absorbing constituents, namely the chromophores, so that paper reflects more light [3].

Light interacts with paper or pulp sheets in various ways. It may pass through, be absorbed and converted into heat, be absorbed and released again as lower energy fluorescent light, reflect from the first surface encountered as in gloss, or diffuse through the paper to exit eventually from one side to the other as shown in figure A.1. Only the light that actually penetrates the sheet can experience absorption and can influence the papers colour in general and brightness in particular.

Gloss, a mirror like first-surface reflectance, and fluorescence are two optical interactions which complicate the measurement of brightness.

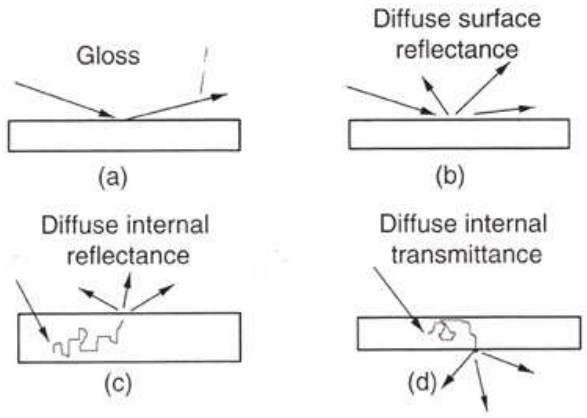

Figure A.1: Different types of light interactions with paper [3].

A.2 Brightness and chromophore concentration

The reduction in chromophore concentration is not proportional to the change in brightness but can be calculated easily from the brightness by applying the

Kubelka-Munk equation [3]

$$\frac{B}{100} = \ 1 + (k/s) - \sqrt{2(k/s) + (k/s)^2}$$

where B is the brightness in percent; s, the scattering coefficient, indicates the likelihood that an optical discontinuity will cause light to change direction within some increment of its diffusion path, and k, the absorption coefficient, is proportional to the chromophore concentration. Figure A.2 illustrates the relationship between brightness and the k/s ratio.

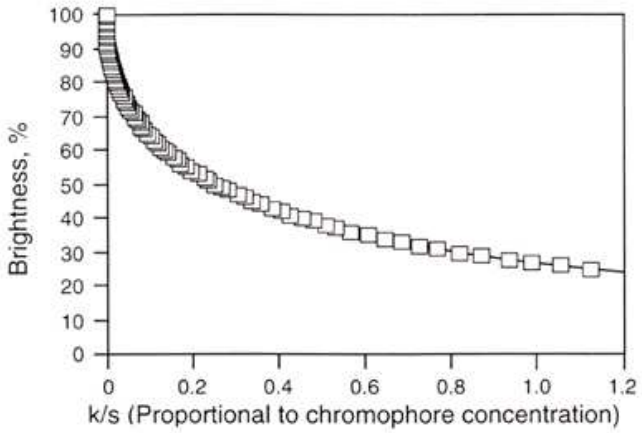

Figure A.2: Relationship between brightness and chromophore concentration [3].

A.3 Brightness standards

Over the years, several methods for measuring brightness have been developed and used as standards. Standardization means that the property being measured is defined. Brightness standards such as $TAPPI$ and ISO were defined in terms of wavelength distribution function, a specific type of instrument, and a calibration routine.

Differences between $TAPPI$ and ISO standards can be summarized as follows [3]:

- ISO brightness is axially symmetric, but $TAPPI$ brightness is sensitive to both machine and cross directions.

- ISO brightness does not consider most of the gloss; $TAPPI$ brightness eliminates nearly all the gloss.
- ISO brightness is based on absolute diffuse reflectance; $TAPPI$ brightness is based on relative directional reflectance.
- $TAPPI$ brightness measures the reflectance at a single illumination angle of 45°; ISO brightness includes all but the gloss-excluded angles at an effective illumination angle of 60° from the normal.

A.4 Brightness sensors

Most of present day brightness sensors implement the ISO brightness standard. Cormec, which was introduced by Kajaani in 1978, is one of the most widely used brightness sensors in pulp bleaching industry today [4].

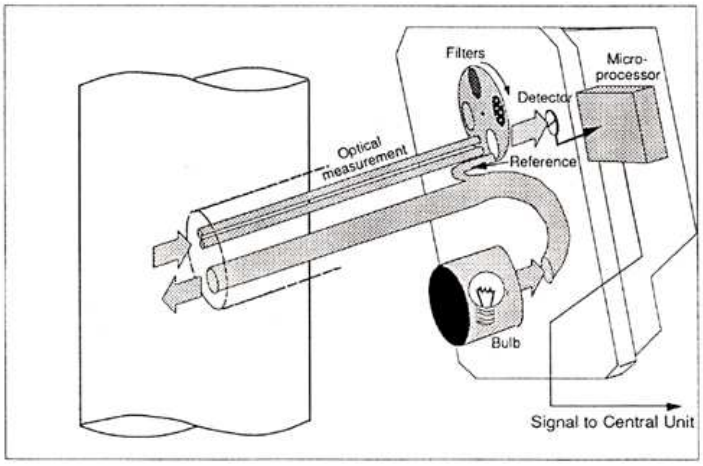

Figure A.3: Cormec measurement [4].

Figure A.3 illustrates the function of the Cormec brightness sensor, where the light being emitted from a halogen lamp is picked up by five fibre optic cables. Four of these cables shine the light into the pulping process through a sapphire lens which protects the cables from the process. The fifth cable which is used as a reference cable, comes directly to the light detection unit.

The light detection unit consists of a motor-rotating disc which has four light filters for red, green, blue, and infrared. There are two light paths that pick up the light being reflected, refracted, absorbed, and diffused from the process. The short

light path is one fibre optic cable mounted very close to the light-emitting cables. The long light path consists of four fibre optic cables mounted further away from the four light source cables (the light paths are not shown in the figure).

The light coming back from the two light paths is sent through the rotating filter wheel to the light detection unit and is converted to an electrical signal. Based on the electrical signal and the reference light the raw brightness is calculated. Several raw brightness measurement can be obtained from the Cormec sensor.

Appendix B

Test and Implementation Issues

B.1 Test and experiment details

Process operators at Irving Paper mill usually control the mechanical pulp bleaching process manually by interacting with the Honeywell *TDC3000 DCS* system. The *TDC3000 DCS* system provides the human machine interface (*HMI*) facilities and the basic control infrastructure, which handles and controls all primary processes in the bleaching process (such as pulp flows and chemicals dosages). A control technology prototype has been designed to implement the designed *DMC* controller in the real peroxide bleaching process at Irving Paper mill. The technology has been implemented in the mill by integrating a *PC* system with the *TDC3000 DCS* system, so that the control program can acquire to the bleaching process parameters in real time. The connection between the control technology and the *DCS* system has been achieved by utilizing the *PI-API* client-server service provided by the *DCS* system.

Since the control technology was designed to test some basic objectives and not to automatically control the bleaching process, it is only allowed to read the bleaching process variables and to calculate the corresponding optimal hydrogen peroxide dosage. Then the process operator can either follow the peroxide dosage recommended by the control technology, or use his experience to manually control the bleaching process. In other word, the developed control technology works as an advisor to the bleaching process operators. Figure B.1 demonstrates the *DMC* control technology implementation at Irving Paper mill.

The Microsoft visual *C++* development environment was used to develop the control technology. *C++* libraries from National Instruments which provide mainly the linear algebra functions and the graphic user interface ActiveX controls, were also used. The control program simply reads all the necessary bleaching process variables to calculate the optimal peroxide dosage at each sampling instant. Then the different process parameters are plotted on line and stored in a file for later processing and review.

Basically the control program was designed based on the single document interface *SDI* application, which offers a lot of flexibility from both the user and the designer points of view. Figure B.2 shows the control program main window and its controls. The control program mainly consists of three parts: the application

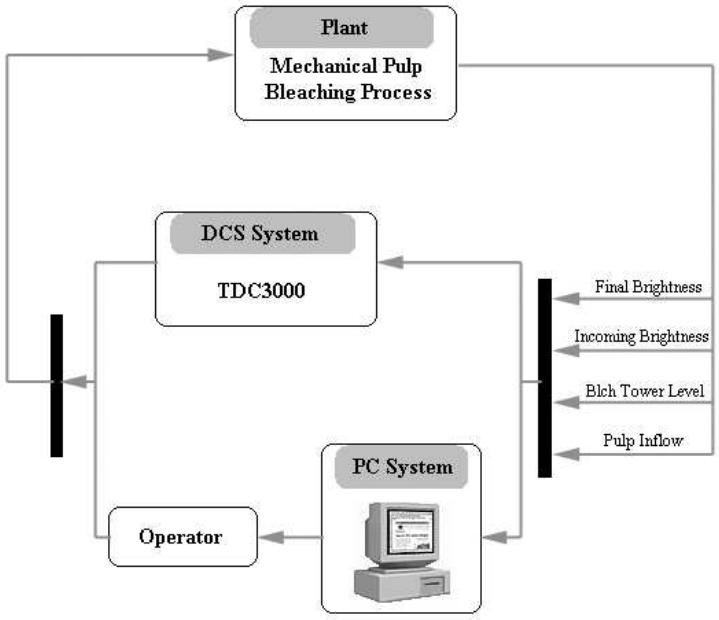

Figure B.1: The *DMC* control technology implementation at Irving Paper mill.

and its graphic user interface (*GUI*), the database, and the run time engine.

B.1.1 The graphic user interface (*GUI*) part

The basis of the control program is the single document interface *SDI* application. The *SDI* application is based on the view/document architecture, where the document is the abstract representation of the data being handled in the application. The view is the visual representation of the date which allows the user to interact with the application efficiently. Figure B.3 demonstrates the design scheme of the control program in terms of its *GUI*, and the relationships between the different constructed objects.

There are four dialog boxes in the application. The application has been designed so that the view object creates two kinds of dialog boxes to enhance the user interaction.The first three dialog boxes are modeless ones which allow the user to work elsewhere in the application while the dialog is active. Their main function is to show the plots of the bleaching process variables online, i.e., bleaching chemical dosages, pulp flows, and pulp brightness. The forth dialog box is a modal one, where the user cannot work elsewhere in the same application until the dialog

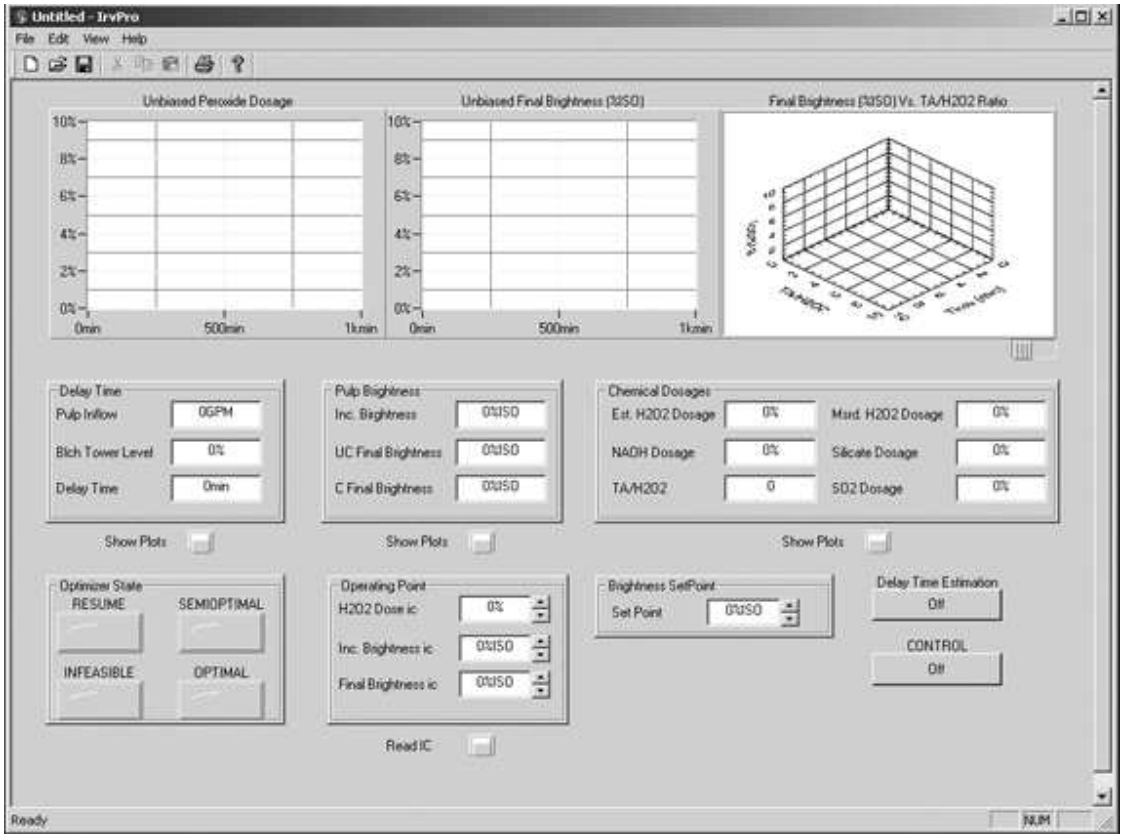

Figure B.2: The *DMC* control technology main window.

is closed. This dialog box allows the user to enter the parameters of the *DMC* controller.

The dialog boxes can be displayed by clicking on the corresponding "ShowPlots" button as can be seen in figure B.2, where there are three different categories of edit controls (in the middle raw of controls in the main window) to show the numerical values the bleaching process variables at each sampling period.

B.1.2 The database and run time engine parts

The variables of the control program have been organised in four structures, where each of the structures is associated with one type of the process variables. The document object contains all the structure and is responsible of handling the flow from/to the hard-disk of the *PC*. Figure B.4 demonstrates the relationship between the document object and the run time engine of the control application.

The run time engine which is considered to be the kernel of the control technol-

ogy, is mainly responsible for generating the optimal control action (i.e., the optimal peroxide dosage). The run time engine is mainly a dynamic link library (*DLL*) which hides the main control and optimization algorithms used in the *DMC* controller. The control and optimization algorithms are encapsulated in a class called IrvMath which is inherited from the National Instruments math class CNIMath. The functions in IrvMath class are structured in two types of access levels. The first one is the public access type, which the application can access. The delay time estimation and the *DMC* control algorithms are examples of the public access type functions. The other type is the private access one, which only functions inside the IrvMath class can access. The optimization algorithm and other functions for internal use are examples of this type.

Figure B.5 shows the flow chart of the control algorithm as a programming example. It starts by reading the necessary measurements from the bleaching process and then compensating for the measurable disturbances such as the pulp consistency and the incoming pulp brightness. The future error between set point profile and the free response is estimated and, based on the optimization method being chosen, the optimal control increments vector is estimated. Then the first element of the control increments vector is applied to the real bleaching process after being integrated and the states are updated. This algorithm is repeated at each sampling instant. As far as the optimization algorithm is concerned, it has been thoroughly discussed in chapter four in case the reader is interested in implementing the algorithm.

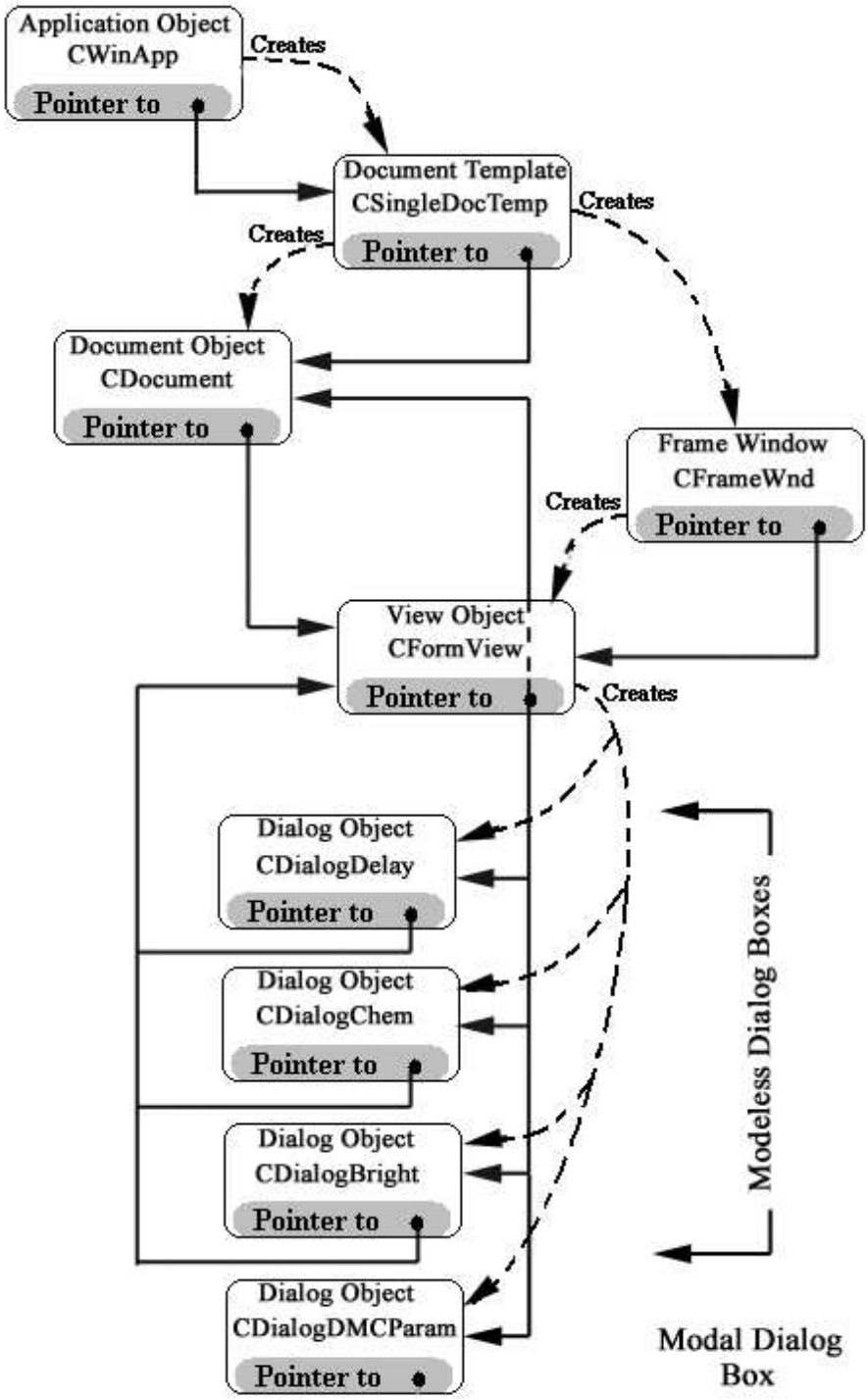

Figure B.3: The *GUI* design scheme of the *DMC* control technology.

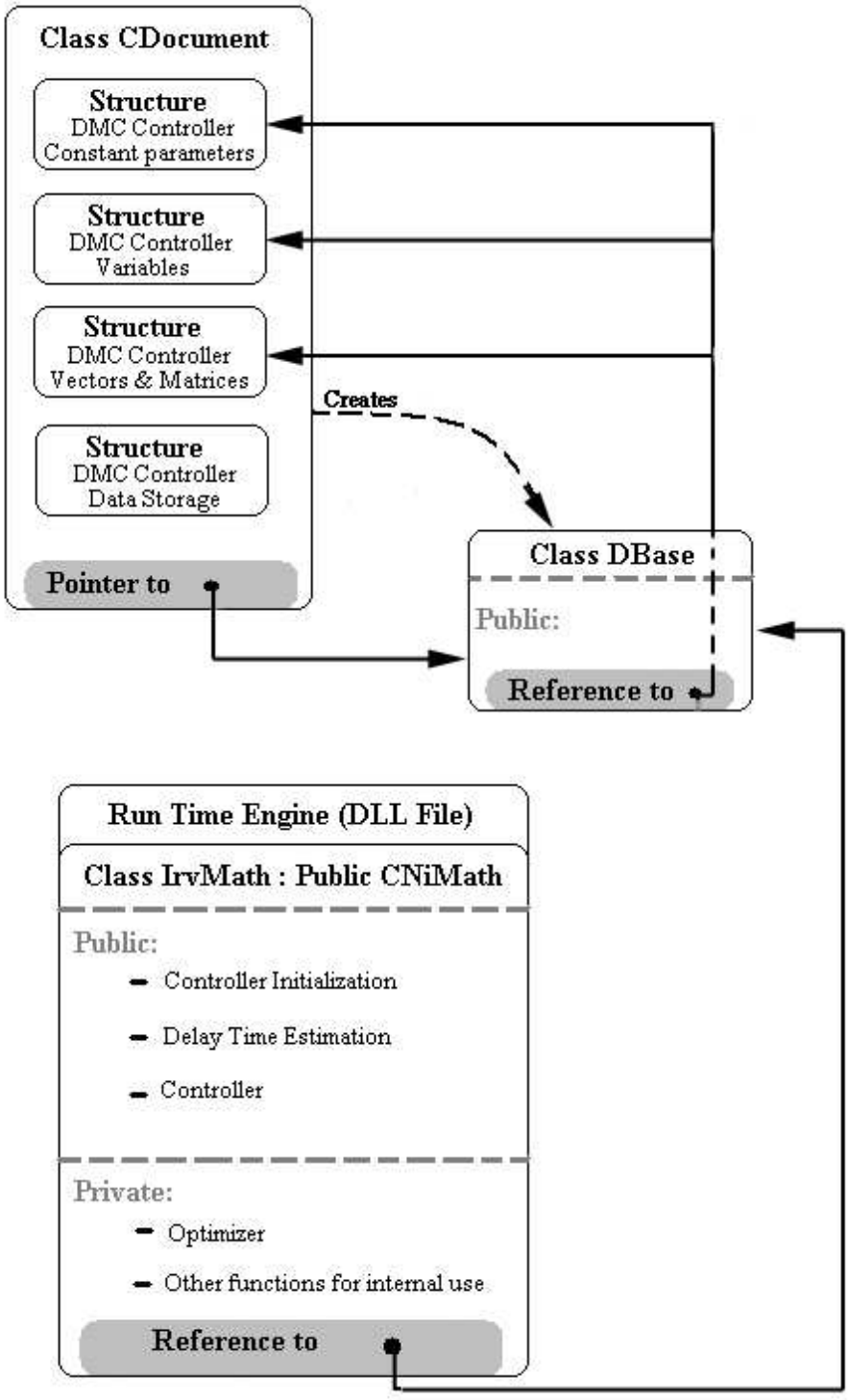

Figure B.4: The run time engine scheme of the *DMC* control technology.

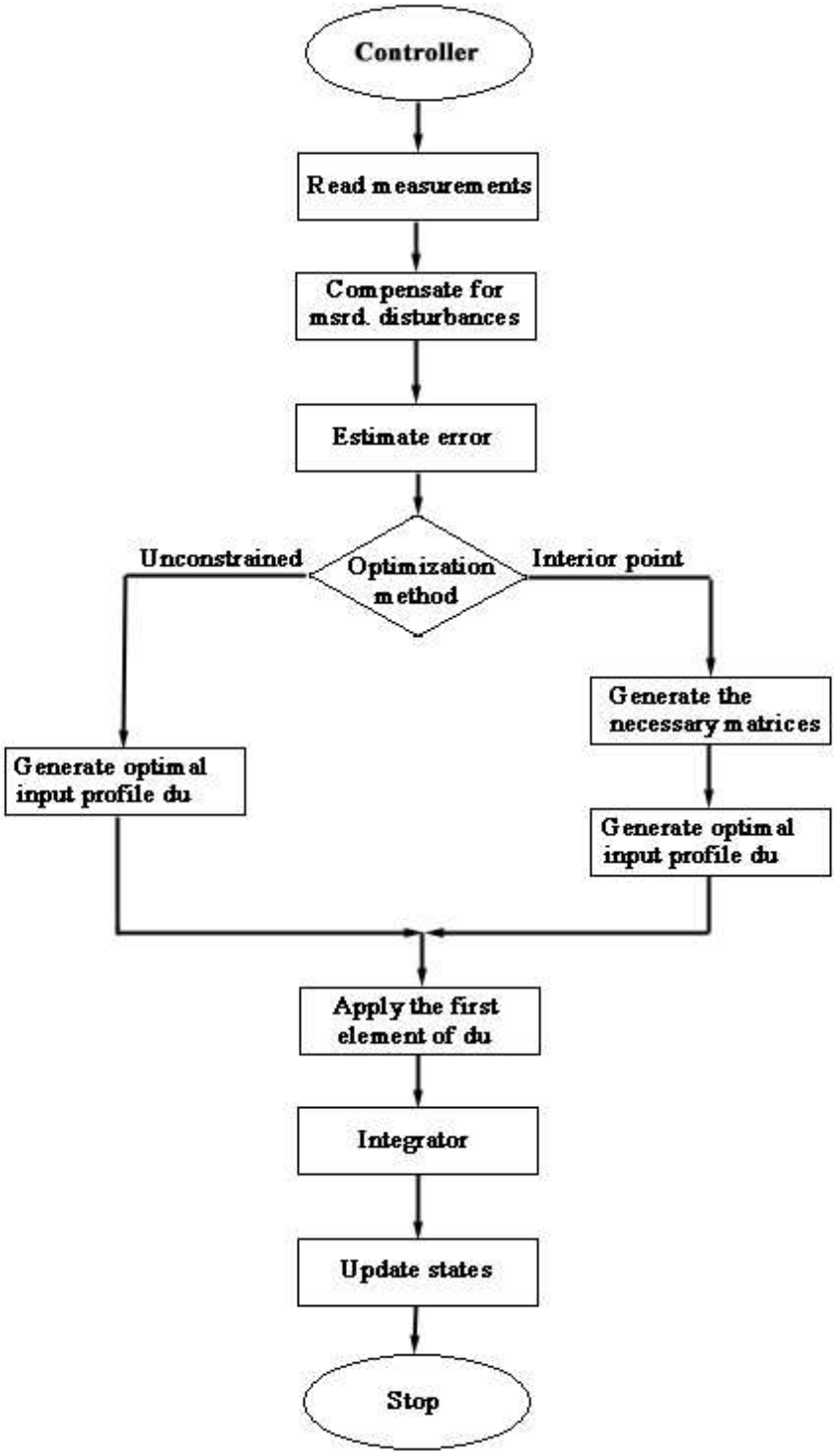

Figure B.5: The flow chart of the control algorithm in the control technology.